



UNIVERSITÀ POLITECNICA DELLE MARCHE  
Repository ISTITUZIONALE

Seismic performance of precast reinforced concrete buildings with dowel pin connections

This is the peer reviewed version of the following article:

*Original*

Seismic performance of precast reinforced concrete buildings with dowel pin connections / Clementi, F.; Scalbi, A.; Lenci, S.. - In: JOURNAL OF BUILDING ENGINEERING. - ISSN 2352-7102. - STAMPA. - 7:(2016), pp. 224-238. [10.1016/j.job.2016.06.013]

*Availability:*

This version is available at: 11566/236346 since: 2022-05-25T11:19:58Z

*Publisher:*

*Published*

DOI:10.1016/j.job.2016.06.013

*Terms of use:*

The terms and conditions for the reuse of this version of the manuscript are specified in the publishing policy. The use of copyrighted works requires the consent of the rights' holder (author or publisher). Works made available under a Creative Commons license or a Publisher's custom-made license can be used according to the terms and conditions contained therein. See editor's website for further information and terms and conditions.

This item was downloaded from IRIS Università Politecnica delle Marche (<https://iris.univpm.it>). When citing, please refer to the published version.

(Article begins on next page)

# SEISMIC PERFORMANCE OF PRECAST REINFORCED CONCRETE BUILDINGS WITH DOWEL PIN CONNECTIONS

Clementi\* F., Scalbi A., Lenci S.

Department of Civil and Building Engineering, and Architecture (DICEA)

Polytechnic University of Marche

Ancona (Italy)

\*Corresponding author: [francesco.clementi@univpm.it](mailto:francesco.clementi@univpm.it)

**Keyword:** precast concrete structures, deformable connections, dowel pin, nonlinear static analysis, nonlinear incremental dynamical analysis, lumped plasticity, diffused plasticity, seismic risk index.

## Abstract

A key aspect in determining the seismic performance of industrial Precast Structures (PS) are the connections between precast elements. The main issue is the capacity of beam-column connections to allow relative displacements without losing beam seating, and to transfer lateral horizontal forces from the beam to the column, without losing load carrying capacity. Referring to a case study based on an industrial PS located in Italy, this work critically investigates the influence of different variables on the connection behaviour, as well as the results of the different safety assessment approaches. Attention has been paid to provide a comparison between different (linear and nonlinear, static and dynamic) analyses with both lumped and diffused nonlinear models. The analyses highlight the importance of the connection between members in the seismic upgrade of existing PS, and the minor role of the mechanical slenderness of the column when considering weak connections.

# 1 Introduction

The recent seismic events and the importance of the prevention, grown in the last few years, have highlighted the necessity of assessing the capability of the existing building heritage to sustain earthquakes, in order to improve the average safety level of the population. The adequate modelling of existing Reinforced Concrete (RC) frames is a crucial issue, related as well to the maintenance and to the structural upgrading possibility. The evaluation of the seismic vulnerability of existing buildings has a key role in determining and reducing the impact of an earthquake [1], in particular in precast concrete structures which have suffered severe structural damages. The example is the last earthquake in Emilia Romagna (Italy) in 2012 [2–4].

There are precast industrial buildings from different periods, designed with different codes and located in different seismic areas, which have experienced earthquakes in Europe and the USA [5–9]. The main causes of Precast Structures (PS) damages under seismic actions are connection failure, insufficient ductility, stiffness and strength of the columns, insufficient roof stiffness or slab system. In particular, the absence of adequate connections between structural elements is a very common weakness, which determines the worst collapses and damages. In most cases, an effective beam-column connection does not exist, and the link is guaranteed exclusively by friction forces [10], which of course are not reliable. The frictional connections are typical of existing PS exclusively designed for vertical loads, in zones that in the last decades have been identified seismically hazardous [11].

The dowel system is one of the most common beam-column connections in some areas recently considered as seismic. It is a mechanical device allowing the transmission of horizontal actions [12], and it generally consists of one or more steel dowels embedded in the column and inserted in a beam hole, filled with mortar. Numerical models of PS usually implement this kind of connection as hinge, fixed between structural elements, and it is considered strong enough to avoid failure during earthquakes.

In the literature there are not so many studies on the dowel capacity influence on the overall spatial responses of the structures, on its seismic vulnerability and, more generally, on the seismic risk: one of the most important works is [13] where the concept of robustness of PS is studied. Indeed, several researchers have analysed only a singular dowel pin connection through FEM, but without a global seismic analysis. Recently, significant experimental and numerical researches on the seismic behaviour of new PS with dry pinned connections were conducted in the framework of two European projects: the “Growth” FP5 project, “Precast structures EC8: Seismic behaviour of precast concrete structures with respect to Eurocode 8 (Co-Normative Research)” and the FP7 project, “SAFECAST: Performance of innovative mechanical connections in p.c. structures under seismic conditions”. The former project focused on the overall nonlinear behaviour of structures with several types of connections and on the global ductility that can be attained [14,15]. The last one focused on the experimental investigation (monotonic, cyclic and dynamic) and the analytical modelling of typical mechanical, dry connections that are used in PS, including beam-column joints [16]. More recent studies [10,12,17,18] were also aimed at developing

a specific procedure for the estimation of dowels capacity. In [11] some considerations on the influences of the neoprene beam-column connections are presented, taking into account the elastic deformation of the rubber on two single story/single-span structures. Only the presence of neoprene between beam and column and not in the secondary elements of the roof, is modelled. In Negro et al. [19] a full-scale three-storey PS was subjected to a series of pseudo-dynamic tests. The behaviour of various parameters, traditional as innovative mechanical connections and the presence or absence of shear walls along with the framed structure were investigated. The main conclusion is that the failure of precast industrial buildings, due to loss of support, can occur due to seismic forces even at medium/low intensity because of low resistance of beam-column connection. These considerations have been elaborated directly through capacity equations when the capacity design is not applicable, as in the existing structures.

The dowel pin connection behaviour is quite complex: it is influenced by the behaviour of different materials (concrete and steel), by the contact among elements (e.g. column concrete-dowel and mortar-dowel), as well as by jointed structural elements (e.g. rotational capacity of beam and column). Moreover, as observed in [16], in many countries (USA, New Zealand, Japan, Australia etc.), rigid connections are preferred for beam-column joints, while in Europe (Italy, Greece, Spain, Portugal, Slovenia etc.) and elsewhere (Turkey, Armenia etc.), simple dry pinned connections are traditionally used in frame type buildings. The Italian code [20,21] underlines the importance of the assessment of connection performance, but it does not give a clear indication of the way to do it, considering the deformability and limit resistance of the dowel pin. With the exception of some guidelines in Japan [22], in the USA [23] and in Italy [24], there is no complete code guidance in response to the existing (industrial) PS with deformable connections. In Europe, the codes are just beginning to tackle the problem with Eurocode 8 [25], major information on this issue is contained in [26,27] with some appropriate capacity equations to this problem. Today, sufficient information is available to obtain a realistic model of these connections and it is possible to determine a correct vulnerability PS index.

One of the most common and serious PS damages due to an earthquake is the failure of the beam-column connection [5,6,9,28]. Few research projects [2,11,28–31] have been devoted to the 3D response of existing industrial PS. This situation is very relevant especially in Italy, because between the 1950s and 1990s a large number of constructions built in many industrial districts are nowadays often exposed to high levels of seismic risk. A description of the typologies of reinforced concrete PS present in Italy is reported in [2,28,31] and also in Sect. 2 of [11]. This is the reason why the assessment herein proposed is performed by a rigorous methodology, collecting many accurate data on the buildings characteristics and analysing them by sophisticated analyses, i.e. nonlinear static and incremental nonlinear dynamic analyses (I.D.A.). Finally, the peculiar weakness of the single dowel connection is shown by the case study.

Based on sensitive analyses our main goal is to investigate the influences of:

- a) the choice of the capacity equations to evaluate the resistance of the dowel pin; in order to have a better perception of the existing situation of Italian precast RC buildings designed with the CNR 10025/84 [32] and CNR 10025/98 [33];
- b) neglecting “*a priori*” possible ruptures of the dowel pins;
- c) the types of analysis, i.e. linear and nonlinear, static and dynamic, in terms of seismic index risk;
- d) the choice of the nonlinear model, such as lumped and diffused plasticity;
- e) the Knowledge Level (KL) which depends on the knowledge of the structures and the resistance of their material (see Table 3.1 of [34]).

## 2 The case study

One-story industrial buildings represent the most common form of precast construction in central and northern Italy, most of them severely damaged during the last earthquakes. The earthquakes in Emilia-Romagna (2012) caused damages mainly to industrial PS with a huge economic loss: it has been roughly estimated that the direct economic damage reaches about €1 billion, while the induced economic damage reaches about €5 billion [28].

In order to clarify the genesis of the major structural deficiencies of the traditional Italian RC precast facilities affected by earthquakes, a brief introduction of the past and current design practice is presented. Detailed explanations of codes evolution are reported in [1,35] for RC structures and in [28,30,31] for PS.

### 2.1 Past and actual design practices

Taking into account the last 60 years, the Italian building stock could be split into three periods: from 1962 to 1987 (poor general rules for RC structures), from 1987 to 2002 (first provisions for PS) and 2003 to present (appropriate design code including a specific chapter on PS).

Starting from 1962, Law 1684 [36] and integration Law 1224 (1964) [37] only specify the horizontal actions to consider in seismic zones in Italy, without any particular requirement for PS. In 1965, the Circ. M. LL.PP. n. 1422 [38] forbade the use of horizontal joints without mechanical devices if the ratio  $V/N$  was larger than 0.35 (where  $V$  is the maximum value of the shear force,  $N$  is the expected axial compression force).

The first specific regulations for PS were in the D.M. 1987 [39], which pointed out the role of the connections, considering the transition construction phases. The requirements for structural elements and for connections design are still limited; it is forbidden in seismic zones to use beam-column connections transferring horizontal forces by friction alone. The only prescriptive provision is given for the width of the beam-to-column support not smaller than  $8\text{cm} + L/300$ , where  $L$  is the clear beam span in centimetres.

Finally, more detailed suggestions on PS are given in 2003 [40] but were compulsory only for infrastructures or strategic buildings. The current Italian code [20] gives more attention to PS than has been given in the past Italian codes, adopting some Eurocode 8 regulatory provisions [25] about the precast concrete structures in Europe, underlining the

importance of the connections. It required to ignore the friction resistance in evaluating the connection resistance between primary and secondary elements.

## 2.2 Geometry and materials

The reference building analysed herein, has a simple and geometrically regular structural scheme (**Figure 1**), which is typically for RC single story precast industrial structures. This building, located in the centre of the Italy, was erected between the end of 1960s and the end of 1970s. It is representative in terms of typology and dimensions, of the industrial buildings present on the territory. To obtain a realistic evaluation of the vulnerability, a great deal has been carried out to determine the most important structural characteristics, by means of a thorough examination of the available technical documentation and many in-situ visits.

The structure has a rectangular plan that covers an area of about 28800 m<sup>2</sup>, with the longest side equal to 240 m and the shortest one equal to 120 m (**Figure 1**). It is characterized by rectangular nets of columns of 20 m x 10 m and the columns height, measured from the industrial floor, is equal to 8 m, with a square cross-section of 0.6x0.6 m<sup>2</sup>. The first part of the structure was built in the late 1960s (see dark grey in **Figure 1**), whose columns were cast on site, and later expanded in the early 1970s, whose columns were made in a factory followed by a verification of materials and reinforcement (see light grey in **Figure 1**). Differently, the roof beam is always factory made with good materials and reinforcement. The distributions of the internal rebar of the columns in the central zone of the building are reported in **Figure 2**.

The infill walls are made of metal corrugated sheets. The beam-column connections are made of steel dowels, with a diameter equal to 22 mm and steel type FeB38k [1]. Differently, the secondary beams are connected to the principal ones by dowels of 16 mm of diameter of the same steel type (**Figure 2**). The foundations are made of plinths (with piles) connected by perimeter curb, and at the ground level, there is a reinforced industrial floor. These characteristics permit one to consider the columns fixed at the zero level (**Figure 2**) of the industrial floor and to neglect any effect due to seismic input asynchrony at the base of the different columns. The covering structure is of shed type and it is made by pre-stressed RC tiles, which are simply supported by the beams. The horizontal connection is guaranteed by friction forces only.

In **Table 1**, the mechanical parameters considered in the modelling of the structure are reported and they refer to a damage section. It is worth noting that average values, with respect to typical values of precast concrete during the construction time, are considered. For the rebar inside the columns and beams, the original design drawings and tables are obtained.

The loads on the roof are very heavy due to a production plant completely suspended and attached to the cover.

The available data permit to achieve a restricted Knowledge Level (KL1), classified in the Italian Seismic Code [20,21] as LC1, corresponding to a Confidence Factor (CF) equal to 1.35, that is the same approach adopted in Eurocode 8 [25].

Two different connections between column and beam elements are considered, named dowel pin *DP1* and *DP2* depending on the different  $f_c$  value of the columns. Another connection, named dowel pin *DP3*, between main beam and joists is considered (**Figures 1-2** and **Table 1**). The distance, evaluated in the direction of the beam elements, with respect to the side (**Figure 2c**) is about 150 to 200 mm for the columns and is about 100 to 150 mm for the beams. From **Figure 2c** it is possible to observe that the weak connection is between primary and secondary beams, and care should be used in modelling this dowel pin.

### 3 Shear strength of dowel connection

Two main cases of dowel interaction are offered by literature. The simplest one is a one-sided plain dowel. The bar is embedded at one end and is loaded by shear force acting along the joint face (see **Figure 3**). The second case, i.e. double-sided plain, is a dowel pin embedded in elements on each side of joint and plastic hinges will ultimately be formed on each side (see **Figure 4**). The failure of these connections is assumed to take place when such a mechanism is formed.

Various failure modes are possible depending on the strength, dimension and position of the dowel pin: steel shear failure, concrete crushing failure or steel flexural failure (combined steel/concrete failure). A weak bar in a strong concrete element might fail in shear of the bar itself. A strong steel bar in a weak element or placed with a small concrete cover, will more naturally result in spalling of the element itself. However, when the bar is placed in well-confined concrete, the dowel pin normally fails in bending by the formation of a plastic hinge in the steel bar (**Figure 3b-4b**). The same occurs when the spalling effects are controlled by properly designed spalling reinforcement.

It is difficult to establish the nature of the connections of the case study: they could be one-sided or double-sided dowels. Precisely, the pins are surely without end anchor but in some cases mortar ground to fill the hole (**Figure 4b**) is present. This means that the axial deformations of the dowel may play an important role also activating the double-sided dowel rupture **Figure 4**.

A sensitivity study (reported in **Sect. 4**) is carried out in order to investigate the main parameters that influence the shear strength of the dowels connections. The mean values of the materials strength are used in all the relationship considered.

#### 3.1 One-sided dowel pin

In this section the reference formulas taken from the literature, which provide the shear strength of the one sided-dowel connection are reported.



The CNR 10025/84 [32] provides a formula to evaluate the monotonic shear strength of the dowel connection. According to this code the connection shear strength is equal to:

$$V_{Rd} = c \cdot d_b^2 \sqrt{f_{yd} f_{cd}}, \quad (1)$$

where  $d_b$  is the dowel diameter,  $f_{cd}$  is the concrete design compressive strength,  $f_{yd}$  is the dowel design yielding strength and  $c$  is equal to 1.2 (without confinement) or equal to 1.6 (with confinement). The confinement effect refers to the presence of compressive stresses, perpendicular to the shear direction (see Figure 3.2.4.1 of [32]). In this case, the effect of confinement is not considered since the presence of an effective contact area between beam and column is plausible only in the principal frame direction. In the other direction only the beam's web is in contact on the column top end with a limited zone. This formula is valid if the eccentricity ( $e$ ) of the shear force (see **Figure 2**) is less than half of the dowel diameter ( $d_b$ ). The CNR formulation does not consider the influence of the concrete cover on the connection shear strength, because it supposes that the connection failure always occurs for steel flexural failure. This formulation is derived in [41], when the phenomenon is analysed by means of the plasticity theory. Since concrete and steel reach a plastic behaviour, the problem can be analysed by considering the dowel actions as a pile resisting as Winkler's material (the concrete). The fact must be stressed that in the analysed case the shear force eccentricity is less than half of the dowel diameter.

According to Vintzeleou and Tassios [42] there are two possible dowel connection failure: the steel flexural failure based on the same model of CNR, and the concrete spalling based on equilibrium of system forces in cracked reinforced concrete. The two mechanisms depend on the concrete cover size in the direction of the load (frontal cover) and in the perpendicular direction (lateral cover) with respect to the dowel diameter. The steel flexural failure occurs when the concrete covers are greater than 6–8 times the dowel diameter. If the shear force eccentricity is negligible, the connection shear strength is equal to:

$$V_{Rd} = 1.3 d_b^2 \sqrt{f_{ys} f_{cc}}, \quad (2)$$

where  $f_{ys}$  is the yield stress of the steel and  $f_{cc}$  is the concrete compressive strength, 1.3 the coefficient that considers the influences of distance to free edges (see Tab. 8-1 and Figure 8-17 of Fib n.43 [26]). If the concrete cover is lower than 6 to 8 times the dowel diameter, the strength of the connection is related to the concrete failure rather than to the dowel crisis (concrete spalling). Depending on the ratio between the concrete cover in the load direction (frontal cover  $c_F$ ) and in the perpendicular direction (lateral cover  $c_L$ ), a bottom spalling (i.e. the failure of the frontal cover) or a side spalling occurs. For low values of  $c_L/c_F$ , a side spalling occurs and the connection shear strength is equal to:

$$V_{Rd} = 2 \cdot d_b \cdot b_{ct} \cdot f_{ct}, \quad (3)$$

where  $b_{ct}$  is the net width of the concrete section, evaluated as the section width (normal to the load) minus the diameter of the dowels, and  $f_{ct}$  is the concrete tensile strength. For high values of  $c_L/c_F$ , on the other hand, a bottom spalling occurs and the connection shear strength is equal to:



$$V_{Rd} = 5 \cdot d_b \cdot c \cdot f_{ct} \cdot \frac{c}{0.66 \cdot c + d_b}, \quad (4)$$

where  $c$  is the frontal concrete cover. The concentrated reaction splits the element, but the spalling can be controlled by reinforcement designed to establish an equilibrium system in cracked reinforced concrete. This means that eqs. (3) and (4) can be excluded if there are reinforcements.

Different formulas have been proposed for cyclic loads and eccentric force by Vintzeleou and Tassios [43]. In the existing RC precast buildings there is at least a thin neoprene film. So that there is a low eccentricity for the shear force and the only equation valid for cycling load is used:

$$V_{Rd} = 0.65 d_b^2 \sqrt{f_{yd} f_{cd}}, \quad (5)$$

which is the eq. (2) reduced by a factor 0.5.

For the Fib n. 43 [26], when the dowel pin is not very weak with respect to the surrounding concrete, the steel bar fails when a plastic hinge appears in the cross-section with the maximum bending moment. This corresponds to the steel flexural failure mode which is associated, as reported in the introduction of this section, to a significant dowel settlement bar that crushed under the high compressive stresses (**Figure 3**). With reference to a one-sided plain dowel, without end anchor and loaded by shear along the joint face with no eccentricity, the monotonic shear capacity is equal to:

$$V_{Rd} = \alpha_0 d_b^2 \sqrt{f_{cd} f_{yd}} \quad (6)$$

where  $\alpha_0 = \sqrt{\beta_c/3}$ , is taken equal to 1.0 like recommended by the Fib n. 43. In the previous,  $\beta_c$  is a factor that considers the tri-axial local state of stress of concrete. In [41] the shear capacity of one-sided dowel pin was evaluated with  $\alpha_0=1.16$ .

According to [44], the shear displacement  $s_{max}$  needed to activate the shear capacity (see **Figure 5**) can be estimated starting from a critical value of the pin plastic hinge inclination  $\theta_{crit}$ . Assuming that the critical inclination has to be proportional to the curvature of the critical section once the yielding is reached, it can be estimated as:

$$\theta_{crit} = k_r \frac{\varepsilon_{sy}}{d_b}, \quad (7)$$

where  $\varepsilon_{sy} = \frac{f_{ys}}{E_s}$  is the yield strain and the  $k_r$  is the factor that considers the curvature distribution, which was experimentally determined and was found to be about 1.75. However, the experimental basis was rather limited and this value is uncertain. Finally, the shear displacement needed to form a plastic hinge can then be determined as

$$s_{max} = \theta_{crit} x_0, \quad (8)$$

where  $x_0$  is the distance from the joint face to the plastic hinge, found as

$$x_0 = \frac{V_{Rd}}{3\alpha_0^2 f_{cc} d_b} \quad (9)$$

For the Model Code 2010 [45] the resistance of the dowel pin is calculated with

$$V_{Rd} = k_2 A_s \sqrt{f_{cc} f_{ys}} \leq \frac{A_s f_{ys}}{\sqrt{3}} \quad (10)$$

where  $k_2=1.6$  and  $A_s$  is the dowel area. The shear-displacement relationship is given by

$$V_v = V_{Rd} \left( \frac{s}{s_{max}} \right)^{0.5} \quad (11)$$

where  $s_{max}=0.1 \div 0.2 d_b$ . In **Figure 5** the following main notation is used:

$$\beta_E = \left( \frac{E_c}{8 \cdot E_s \cdot I_s} \right)^{0.25} \quad (12)$$

where  $E_s$  and  $I_s$  are modulus of elasticity and second moment of area of the bar, respectively.

According to Soroushian et al. [46], the shear strength for the dowel bars if the force is applied against the concrete core (i.e., steel-flexural failure), is:

$$V_{Rd} = 0.5 f_b (0.37 \gamma d_b - c')^2 + \frac{0.45}{\gamma} f_{ys} d_b^2 \left( 1 - \frac{T^2}{T_y^2} \right), \quad (13)$$

where  $\gamma = \sqrt[4]{\frac{E_f}{k_f d_b}}$ ,  $k_f$  is the concrete foundation modulus ( $\sim 271.7 \text{ MPa/m}$ ),  $f_b = 37.6 \left( \frac{\sqrt{f_{cc}}}{\sqrt[3]{d_b}} \right)$  is the concrete bearing strength,  $c' = 0.05 \cdot \frac{f_{ys} d_b}{f_{cc}} \cdot \sin \alpha$  is the length of the crushed concrete zone and takes into account the inclination  $\alpha$  of the bar,  $T$  is the dowel bar axial force,  $T_y$  is the dowel yield axial force. When the force is applied against the concrete cover [47] (i.e., concrete spalling), the same authors provided an equation to calculate the strength of connection:

$$V_{Rd} = 0.83 \psi b_{ct} f_{ct}, \quad (14)$$

where  $\psi = \pi / \left( 2 \sqrt[4]{\frac{k_f d_b}{4 E_s I_s}} \right)$  is the distance from the crack face to the inflection point (see Figure 12b of [47]).

### 3.2 Double-sided dowel pin

When the plain dowel pin is embedded on the two sides of the joint, a point of deflection develops at the joint interface. Two plastic hinges (**Figure 4b**) will develop simultaneously at a distance  $x_{0,i}$  from  $i$ -element and the joint interface. The different values of  $x_{0,i}$  depend on different strength of concrete on the column and on the beam. If the concrete strength is the same in both elements,  $x_{0,i}$  have equal values.

The case in **Figure 4b** is non-symmetrical: connection has a stronger and weaker side. For a certain shear force, a plastic hinge is formed in the dowel pin at the weaker side, while the dowel still has an elastic behaviour at the stronger side. Hence, the load can be increased further until a plastic hinge is formed also at the other side. However, the stiffness of the

shear connection is reduced by the formation of the first plastic hinge (see also §8.2.3 in Fib n.43 [26]).

The ultimate capacity of the connection is determined by the formation of the second hinge. Therefore, the shear capacity can be calculated with eqs. (1-2,6,10), reported in the previous paragraph, where  $f_{cc}$  must be equal to the higher strength of the jointed elements and without eccentricity.

For non-symmetrical conditions, the shear displacement needed to create the failure mechanism can be expressed by means of the critical angle, eq. (7), but considering in the eq. (8) the distance between the plastic hinges  $l_p$  equal to:

$$l_p = x_{0,1} + x_{0,2} + t_j \quad (15)$$

where  $t_j$  is the width of joint gap, if any.

The associated skeleton curve of typical shear-displacement relationship [26] for a dowel pin with non-symmetrical condition is reported in **Figure 5c**.

However, new formulation is reported in the SAFECAST Project with Negro & Toniolo [48], for the spalling of concrete edges. It is assumed that the shear strength is

$$V_{Rd} = \frac{1.4 \cdot k \cdot d_b^\alpha \cdot h^\beta \sqrt{f_{ck,cube} \cdot c^3 \cdot \psi_{re}}}{\gamma_c}, \quad (16)$$

where  $f_{ck,cube}$  is the characteristic compressive cubic strength of concrete,  $c$  edge distance of the dowel axis,  $h=8d_b$  effective length of the dowel,  $b$  width of the column,  $n$  number of dowels,  $\alpha=0.1(h/c)^{0.5}$ ,  $\beta=0.1(d_b/c)^{0.2}$  and  $k=b/(3c) \leq n$ . In eq. (16)  $f_{ck,cube}$  is expressed in N/mm<sup>2</sup>,  $V_{Rd}$  in N and  $d$ ,  $h$ ,  $c$ ,  $\psi_{re}$  in mm and  $\psi_{re}=1.4$  in the presence of edge reinforcement or  $\psi_{re}=1.0$  in all other cases.

Based on the results of experiments performed in SAFECAST project context [49], modified formulas (5) have been proposed by Psycharis and Mouzakis [16], which account for cyclic behaviour of the realistic beam-to-column dowel connections:

$$V_{Rd,sr} = 1.1 d_b^2 \sqrt{f_{yd} f_{cd}}, \quad (17)$$

$$V_{Rd,lr} = 0.9 d_b^2 \sqrt{f_{yd} f_{cd}}, \quad (18)$$

where  $V_{Rd,sr}$  is the ultimate resistance of the connection if small rotations between beam and column are expected,  $V_{Rd,lr}$  is the ultimate resistance of the connection if large rotations between beam and column are expected.

### 3.3 Dowel connection shear strength for the case study

In this case study, due to the presence of columns cast on site (i.e., Columns 1 and some Columns 2), the presence of adequate stirrups in the upper side of the columns, is not always guaranteed due to the lack or bad positioning. Consequently, excluding "a priori" concrete spalling for *DP1* and *DP2* is not on the safe side. Therefore the error induced neglecting the absence of an adequate reinforcement at the top of the columns is evaluated

in terms of seismic action. The same considerations are valid for the connections between beams (*DP3*) because the spalling cannot be controlled by the longitudinal and transversal reinforcement of the secondary I-beams (**Figure 2**). Furthermore, since there is no certainty in the length of the dowel and in the presence of filling mortar inside the dowel hole, it is difficult to establish the activation of axial deformations like for double-sided dowel pin. Hence, one-sided and double-sided dowel pin mechanisms, are studied in order to establish the range of variation of the risk index at varying of the structural behaviour of the dowel pin connection.

In **Table 2**, the values of the shear capacities ( $V_{Rd}$ ) of dowel pin considered in the modelling of the structure are reported, calculated with the resistance in **Table 1**.

As shown in the **Table 2** the CNR's formula, as well as the Model Code 2010, provides an estimation of the resistance of about 30% lower than that obtained, more recently, from experiments reported in [48]. When the cyclic input is considered, from Tassios-Vintzeleou a half of shear resistance of the dowel pin with respect to CNR and Model Code formulations is observed. Differently, the lower values of the capacity equations are given by the spalling rupture of Tassios-Vintzeleou. This comparison suggests that the CNR gives a bigger value and therefore the existing structures (that in Italy have been designed with CNR formulation) will most likely have problems of resistance of the dowel pins, not only those made between 1960-90s. Furthermore, comparing the formulations of one-sided pins with those of double-sided pins, a bigger resistance is obtained by the former. The CNR formulation gives a resistance of about +10% respect to the new one of Psycharis & Mouzakis. This means that the one-sided dowels, in Italy, may be under-designed if compared to the double-sided resistances. At the end, it is necessary to stress the fact that the Soroushian's formulation for the concrete spalling gives a higher value if compared to the other models that take into account the concrete spalling rupture.

## 4 Seismic vulnerability assessment

In this section, a summary of the major results of the seismic vulnerability assessment of the industrial building illustrated in Sect. 2 is reported. Three models are considered: two of them are constituted only by beam and column elements for which the beam-column connections perfectly restrain the relative horizontal sliding. In *Model 1* the connections are cylindrical hinges, only the bending moment around the horizontal axis is released, while the rotation around the vertical axis is restrained. This typically represents a correct capacity design or the presence of two or more dowel pins. In *Model 2* the connections are spherical hinges, both bending moments are released. This typically represents a configuration with a single dowel pin with higher resistance than the column. The *Model 3* has the same bending joints of *Model 2*, but in addition it has horizontally deformable connections. In all cases, the torsional moment on the beam is released and the rigid motion of the beams around their axes is neglected.

Models 1 and 2 are those commonly used in applications, they are considered as reference to highlight the improvements obtained by an accurate modelling of the connections, as done by *Model 3*.

The effects of cladding panels are not considered in this paper because the infill walls are made of metal corrugated sheets with very low weight/mass.

Modal analysis with design response spectrum, nonlinear static analysis and nonlinear incremental dynamic analysis (I.D.A.), are considered [50]. All structural models have been developed with the same commercial FE program Midas Gen© [51], for both the linear and nonlinear analyses.

The structural model is reported in **Figure 6**. Beams and columns are 1D elements, and the columns are fixed at their base [52]. Rigid links to simulate the eccentricity in the local connections and general links to simulate the dowel joints are used. The masses are distributed along the elements as well as the loads.

For each model the hypothesis of deformable floor in its plane is used, since this is the closer to the real case. The considered industrial building belongs to the “Class II” in the Italian seismic code [20]. This implies that the Limit State of Significant Damage (SLSD, or SLV in Italian) is associated to a demand recurrence period ( $T_{R,D}$ ) of 475 years, which corresponds to an expected peak ground acceleration (P.G.A.) equal to  $0.256g$  ( $a_{g,D}$ ). The other parameters that characterize the elastic response spectrum are (soil type T1 and category of subsoil C are considered):  $S = 1.5$ ;  $T_B = 0.152$  s;  $T_C = 0.456$  s;  $T_D = 1.904$  s. The elastic spectrum only for linear analysis can be reduced by the factor  $q$ . It can vary between 1.5 to 3 for ductile mechanisms, and it is equal to 1.5 for brittle mechanisms, as prescribed by the Italian seismic code [21].

For nonlinear dynamics analysis, three (1-component) 25 seconds artificial spectrum-compatible times histories (TH1, TH2, TH3) have been generated by the software *Simqke-GR* [53]. Seven more (2-components) 25 seconds natural spectrum compatible times histories (see **Table 3**) have been generated with the software *REXEL* [54]. All ten time histories (T.H.) are used as given accelerations at the base of the columns: their spectrum, together with the reference elastic spectrum, are reported in **Figure 7a-b**.

#### 4.1 Modal analysis

In order to assess the dynamic characteristics of the structure, modal analyses were initially performed by considering the three elastics models (*Model 1*, *Model 2*, *Model 3*) with flexible floors. The spatial models have the mean values of resistance for concrete and steel (see **Table 1**). The dowel pin connections are characterized by the elastic part of constitutive laws reported in **Figure 5b-c**.

The natural periods are reported in **Figure 8a**, while the corresponding participation masses are reported in **Figure 8b**. From the latter, as expected (due to the flexibility of the floor) a large number of modes may be necessary to get a total amount of effective masses greater than 85%.

The vertical vibrations are detected but not reported for brevity issue. The first conclusion is that despite the model is able to capture the vertical component of free vibrations, the main modes are always translational and the vertical components born only up to the third mode. *Model 1* and *Model 2* have the main vertical modes with low participation masses about ~34% (3<sup>rd</sup> mode) and ~27% (5<sup>th</sup> mode) respectively. For *Model 3* the influence of the vertical component of vibration is less and the main mode is the 4<sup>th</sup> with participation mass about ~21%. Despite the low participation masses of the vertical modes, as stated in [4,11], the vertical components are important when connections based on friction forces are considered. The variation of the axial force, more significant at the corner columns where the static vertical load is lower, can cause the sliding of the beam on the column and then the building failure due to loss of support.

#### 4.1.1 Dynamic response spectrum analysis

In this section, the seismic vulnerability assessment is made by means of a linear dynamic analysis. According to [20], the effects of the earthquake in one direction are combined with the 30% of the effects of the earthquake in the orthogonal direction. The Complete Quadratic Combination (CQC) for the superposition of the modal effects is considered.

Even though for PS the second order effects can be relevant, the coefficient

$$\theta = \frac{P_{tot} \cdot d_r}{V_{tot} \cdot h} = 0.055 \quad (19)$$

is below 0.1; consequently, according to [20,25], the second order effects can be neglected. In eq. (19)  $P_{tot}$  is the total gravity load acting on the storey considered in the seismic design load combination, and  $d_r$  is the design inter-story drift evaluated considering the elastic spectrum in **Figure 7**. **An accidental eccentricity equal to 5% of the size of the building (measured in the perpendicular direction with respect to the applied seismic action) is also used. The eccentricity is assumed constant in magnitude and direction and is considered for each mass, instead of total mass according to the flexible roof hypothesis.**

The Seismic Index Risk ( $I_R$ ) is evaluated for both ductile and brittle mechanisms with a design response spectrum reduced by a factor  $q=1.5$ . This choice comes from the fact that the dowel pin may lead to a global brittle collapse in correspondence of the structural joints, if not correctly reinforced like in this case study.

The  $I_R$  is computed both in term of PGA or  $T_R$  by means of

$$I_R = \left( \frac{a_{g,C}}{a_{g,D}} \right) \quad \text{and} \quad I_R = \left( \frac{T_{R,C}}{T_{R,D}} \right)^{0.41} \quad (20)$$

It might be worth to keep in mind that  $I_R \geq 1$  corresponds to a safe structure,  $I_R < 1$  corresponds to an unsafe building with respect to the standard of the new buildings.

The values  $a_{g,C}$  and  $T_{R,C}$  in (20) for the SLSD correspond to the seismic action that produces the breakage of a number **(two/three)** of **neighbour** elements such as to trigger a ductile (i.e., bending moment) and/or brittle (shear resistance) mechanisms, and it comes from the dynamic analysis (and in subsequent sections by the nonlinear analysis). For the

considered building the values are  $a_{g,D}=0.256g$  and  $T_{R,D} = 475$  years, that are the design seismic action for a new building (see **Sect. 4**). The exponent 0.41 in (20)b allows comparison between the two  $I_R$  [55]. The use of the Seismic Index Risk  $I_R$  gives the possibility to work, indifferently, with PGA (International country) or  $T_R$  (Italian country) once the value is known.

In the models the mean values of the properties reported in **Table 1** are used to determine the design bending moments  $M_{ED}$  and shear action  $V_{ED}$ . Differently, the design checks [20,21] need moment ( $M_{Rd}$ ) and shear ( $V_{Rd}$ ) resistances which are reduced by the Confidence Factor (CF), this latter depending on the KL as explained in Eurocode 8 [34] and also in the Italian code [20].

For the *Model 3* (case with dowel pins), the main results are summarized in **Table 4**. The Seismic Risk Index ( $I_R$ ), computed by means of (20)b, is always the same  $I_R=0.155$ . Only the concrete spalling model of Tassios-Vintzeleou gives  $I_R=0.11$ . This value is low if compared with the others, it highlights the necessity to work with nonlinear constitutive equations to take into account the softening/hardening effects and not only the peak of resistance. This aspect is also important to make some considerations about the differences (in terms of  $I_R$ ) on the connection ruptures (flexural failure or concrete spalling), which are difficult to capture with linear analysis.

The independence of  $I_R$  on KL is due to the fact that the first elements to break are dowel pins. They activate a brittle collapse mechanism, which interests only the connections between elements (columns/beams and beams/beams) and does not exploit the ductility resources of the columns (which depend on KL).

The previous fact is very important, because it underlines weak connections in the considered building, therefore they deserve careful analysis, major attention, and possibly retrofiting. Incidentally, it is possible to note that this is what happened to various industrial buildings experiencing the recent Emilia Romagna earthquakes [2,3,28–30]. In [28] it shows a significant example of unsuitable design of dowel pin connection: the spalling of concrete cover occurred before the yielding of the dowel (due to small size of the cover and to the lack of dense stirrups close to the supporting zones). The authors observe that the collapse of few (even one) connections can cause the collapse of the whole structure and, consequently, the loss of both lives and inventory.

To have an adequate perception of the approximation level that is introduced by neglecting the limited resistance of the dowel pin, the  $I_R$  for perfect connections is computed for both cases of cylindrical and spherical connecting hinges (*Models 1* and *2*, respectively). The results are summarized in **Table 5**, which report the recurrence period  $T_R$  and the seismic risk index for both the ductile and brittle mechanisms.

The first point to be observed is that the  $I_R$  are always larger than that of *Model 3* (**Table 4**) as expected since the dowel pins were the weak point. The difference in term of  $I_R$  is large and leads to an overestimation (against safety) of the seismic resistance of about



110% for the spherical hinge and about 135% for cylindrical hinge. This highlights, even at a quantitative level, how dangerous it is to neglect the limited resistance of the dowel pin.

The analyses of *Models 1* and *2* highlight the capacity of the structure once the problem of weak dowel pin has been fixed. Actually, it is possible to observe that the columns undergo a ductile break for low values of  $T_R$ , while the brittle mechanisms are not activated. This is consistent with expectations, as the columns are very slender cantilever beams and therefore not stressed by shear.

#### 4.2 Nonlinear static analysis with lumped plasticity

Nonlinear static (pushover) analysis is become the preferred procedure for design and seismic performance evaluation. The construction of the capacity curve for RC structures requires a certain computational effort. The nonlinear static analysis is performed following the N2 method, originally proposed by [56]. Two distributions are considered: the first one proportional to the fundamental modes (namely, "PushMode") in the considered direction and the second one proportional to the mass (namely, "PushMass"). **The displacement, for all the analyses, is recorded in the central node of the roof.**

A lumped plasticity model is considered [57]. In particular, the nonlinear properties are assigned only to the columns and general links. The columns are characterized by elasto-plastic curves for bending moments with nonlinear constitutive law suggested by the Eurocode 8 provisions [34] and limited ductility behaviour (**Figure 9a**). The shear failures have been taken into account by the introduction of shear hinges with elastic-brittle with limited ductility behaviour (**Figure 9b**). The general links are characterized by the nonlinear (ductility limited) law of **Figure 5b-c** when the steel flexural failure is considered. Differently, in the spalling model an elasto-brittle law similar to the shear failures cases is used (see **Figure 9b**). This permits to have the lower bound of resistance of the dowel pins in complete absence of stirrups for the spalling and consequently the upper bound with *Model 1*.

According to [34], the beam and column verifications for the SLSD (Limit State of Significant Damage) consist in checking that the displacement demand could be achieved by structure without the elements reaching their ultimate deformation (ductile mechanism, **vertical drop in Figure 9a**) or their ultimate shear resistance (brittle mechanism, **vertical drop in Figure 9b**). The ultimate deformation of a column/beam is computed in terms of chord rotation ( $\theta_u$ ) following the formula reported in [34] (that is the same of [21]). It is defined as the rotation of the last cross-section with respect to the line connecting this cross-section with the point in which the moment is equal to zero, at a distance  $L_v = M/V$ , where  $L_v$  is the shear span,  $M$  is the bending moment and  $V$  is the shear at the considered cross-section. The check is satisfied if  $\theta_D \leq \theta_C$ , where  $\theta_C$  is the chord rotation capacity, that for SLSD is equal to  $\frac{3}{4}\theta_u$  [20,21].

For the flexural members a biaxial bending with axial interaction is used (NMM), in order to consider the complex interaction between the bending moments of two axes and the axial force, during the transversal load increment.

The elements have also been verified for brittle mechanism if  $V_{Rd} > V_{Sd}$ , where  $V_{Rd}$  is evaluated with the capacity equations (6.2a-b), (6.8) and (6.9) of EC2 [58].

In **Figure 10**, the main results of the pushover analysis for varying capacity models of the dowel pin are reported (*Model 3*, see Sect. 3). Only 7 models are considered (out of the 10 of **Table 2**) because the other 3 curves are superposed with the depicted plots. The main conclusion that can be drawn is that the capacity curves have a sudden jump when few connections are broken, that entails a very low ductility. The formulations of CNR is in the middle of the range, and can be a good balance to evaluate the real resistance of buildings.

The scarce ductility can be even better appreciated by comparing the previous curves with those with cylindrical (named *Model 1* in **Figure 10**) and spherical (named *Model 2* in **Figure 10**) hinges, which have a much larger ductility, due to the localized dissipations at the base of the columns.

To understand the actual vulnerability of the structures, the recurrence time  $T_{R,C}$  and the seismic risk index  $I_R$  are evaluated for all models with dowels pin (*Model 3*). The results are summarized in **Table 6**. For the pushover analysis the recurrence period of capacity (i.e.  $T_{R,C}$ ) is calculated when a little ductile/brittle mechanism is activated in a little number of close columns or dowel pins. This happens when the columns and/or the dowel pins have reached their capacity in terms of cord rotation (only columns) or shear strength (columns and dowels).

The  $T_{R,C}$  (and the corresponding  $I_R$ ) are bigger than those obtained with a linear analysis, as can be seen comparing **Table 4** and **Table 6**. This confirms that it is not a conservative approach. Since in all cases the overall failure of the structure is related to the failure of the dowel pins, the nonlinear static analysis (as the linear dynamic analysis) highlights the primary role played by the connections. **Table 6** gives –indirectly– the error on the seismic vulnerability that the engineers will obtain if they exclude “a priori” the spalling rupture in the dowel pin connections. Comparing the spalling ruptures evaluated with Negro & Toniolo [48] and the steel flexural failure with small displacement of Psycharis & Mouzakis [16], a difference in terms of  $I_R$  about -10% is observed and about -23% comparing the same with the CNR formulation. The latter compared with the Fib n. 43 gives a difference of about 9% in term of  $I_R$ .

Comparing the  $I_R$  in **Table 6** with those reported in **Table 7** (where there are perfect connections, namely *Model 1* and *2*), it is evident that the activation of the ultimate cord rotation of the columns is at  $T_R=35$  years ( $KL=1$ ). This value is little higher of  $T_R=25$  years of CNR 10025/84, but there is a difference of about +15% in terms of  $I_R$ . With respect to the new formulations reported in Psycharis & Mouzakis [16] (for double-sided pin) there is a difference in terms of  $T_R$  of +75%. This comparison shows once more that the connections are the weak point, thus their improvement is necessary prior to proceed with the retrofitting of the other parts of the structure.

As far as the knowledge level is concerned, in the *Model 3*, since the failure occurs due to the connections, the results are independent of KL (just as in Sect. 4.1.1). Thus, in this case, to reach a large KL is useless. Contrarily, when the connections are well designed and the failure is due to the RC columns, it is expected that the larger KL is, the larger  $I_R$  is. This actually occurs for the *Model 1*, where  $I_R$  has an increment of about +20% from KL1 to KL2 and of about +75% from KL1 to KL3. Is not the same in the *Model 2*, where  $I_R$  is independent by KL. In this model, a global mechanism activation is observed (at  $T_{R,c}=250$  years) before reaching a shear rupture in the columns.

It is worth to remark that, in general, at displacements attained at the end of the pushover curves, the second order effects could influence the results. However, in the particular case reported herein, such an effect is not relevant, as also shown by (19). Furthermore, to have a better understanding of this aspect, some analyses with the P-delta effects were conducted. In conclusion major differences are not recorded with respect to the cases with small displacements.

As a final remark it is possible to observe that all the main conclusions drawn with the linear dynamic analysis have been confirmed by the nonlinear static analysis.

### 4.3 Nonlinear dynamic analysis with lumped plasticity

In order to take into account the effects of the earthquake in a more accurate way, nonlinear dynamic analysis is carried out. In particular, a multi-directional Incremental Dynamic Analysis (I.D.A.) is performed. It consists of applying to the structural model, one (or more) ground accelerations, scaled by an amplitude factor. For each value of the increasing amplitude factor, the nonlinear equations of motion are integrated and the maximum displacement is recorded, thus obtaining the nonlinear dynamic capacity curves [59].

A hysteresis model for flexure and shear members needs to be introduced. A modified Takeda-type model is used [60] for columns, due to its ability to provide simple, numerically stable and sufficiently realistic hysteresis cycles. The degrading stiffness is modelled through the parameters  $\alpha_1$  and  $\alpha_2$ , which also determine the amount of energy dissipated during oscillations. In these analyses  $\alpha_1=0.5$  and  $\alpha_2=0.1$  have been assumed, which seems to be a good approximation of the real case [35].

I.D.A. analyses have been done for dowel pin (*Model 3*) with CNR formulation and for infinitely resistant connections (*Models 1* and *2*). The main results in terms of capacity curves (evaluated in the same control node of the previous pushover analyses) are reported in **Figure 11** at varying of T.H.

For the *Model 3*, two (PushMode and PushMass) pushover curves are also reported in **Figure 12**, with the average values of the ten T.H. (natural and artificial) and the corresponding variation in term of standard deviation. The pushover analysis provides a good result if compared to the I.D.A. global response at varying of the T.H.

The pushover curves of *Model 1* and *Model 2* (blue and black lines in **Figure 13**) are always above the I.D.A. curves. This means that, at least in these cases, the I.D.A. curves do not belong to the envelope of the pushover curves or, similarly, that the two pushover

curves are *not* upper and lower bounds for the more realistic (and more difficult to obtain) I.D.A. curves. There are these differences because in the Model 3, in IDA analysis, the ruptures are always in the dowel pins –since the initial step– and the columns are in the linear range. Differently, in the *Model 1* and *Model 2* the columns reached the yielding (different initial part of the curve respect to *Model 3*) but they retain plastic resources up to large displacements. Evidently, in these cases the pushover analysis overestimates the resources of the structure.

The  $I_R$  are evaluated for all models in order to complete the analysis. The model with dowel pin with CNR formulation shows the activation of a local mechanism for a scaled time history corresponding to average values of  $PGA=0.065g$  and of  $T_R = 15$  years ( $I_R=0.243$ ). Referring to the results of **Table 6** a lower value of  $I_R$  about -20% is observed. This result shows that the I.D.A.s provide intermediate results between linear dynamic and static pushover analyses. Differently, for the case of rigid connections (*Model 2*), the  $I_R$  obtained with I.D.A. are similar to those reported in **Table 7**. Since the triggering of a mechanism is in correspondence of an average  $PGA \sim 0.1g$  and of a  $35 < T_R < 40$  ( $0.343 < I_R < 0.363$ ) years for KL1. The same comparison is valid for other KL and *Model 1*. In addition, it has been confirmed that increasing KL does not have particular benefits in terms of  $I_R$  if the mechanism is associated with the dowel pin crises.

## 5 Lumped vs. diffused plasticity

Nonlinear analyses are very sensitive to the techniques employed in geometric and material modelling. Thus, nonlinear static and dynamic analyses with the fiber model were performed [61], with the aim to compare the results with those obtained in **Sects. 4.2-4.3** with the lumped plasticity model. The benefit of the former model is the simplicity of the discretization of the cross-sections with nonlinear fibres. Another advantage of the fibre model is the more accurate moment-curvature relationship and this is traceable along the whole beam element. On the contrary, the fibre model is much more demanding from a computational point of view.

The model of Kent and Park [62] is used for the concrete fibres, while the model of Menegotto and Pinto [63] is adopted for the reinforcement fibres.

In a fibre model, the axial force and the bending moments of the section are calculated by summing up the stress of each fibre. For the shear verifications, in particular for the pushover analysis, the information provided [21] in Sect. C8.7.2.4 is used. In the pushover analysis of the system with n-degrees of freedom the maximum shear at the base  $V_{bu}$  is obtained, so the displacement corresponding to  $V_{bu}$ , i.e.  $d_{cu}$ , is identified. If the demand displacement  $d_{max}$  is minor to  $d_{cu}$  the demand shear in the elements will be calculated at  $d_{max}$ , differently if  $d_{max} > d_{cu}$  the demand shear in the elements is  $V_{bu}$ .

It is important to underline that the same fiber models are used for the nonlinear static analysis and for the I.D.A., while the curves reported in **Figure 5** are used for the dowel pins.

In **Figures 14a-15a**, the PushMass distribution of the nonlinear static analyses is reported for both +X and -Y directions (evaluated in the same control node of the lumped plasticity). It is possible to observe that the nonlinear fiber models (continuous lines) give the same asymptotic behaviour of the lumped plasticity (dashed lines), even if they significantly differ in the central part of the curves. A slightly different behaviour of the linear range is perceptible, due to the initial choice of the shear span  $L_v$ , overestimated (in the linear part) in the lumped plasticity. Similar results are obtained for the PushMode pushover curves, not reported in the **Figures 14a-15a** for a better reading.

To have a better perception of the seismic vulnerability, the points of verification in terms of  $I_R$  for the two nonlinear models in **Figures 14a-15a** are also reported (with dot, square and triangle). The major differences are in *Model 3* with CNR formulation. Here the shear mechanism is triggered at the third step of loading for the fibres model that corresponds to a  $T_R=5$  years ( $I_R=0.155$ ), with respect to a  $T_R = 25$  years ( $I_R=0.299$ ) for lumped plasticity. This means a decrease in terms of  $I_R$  of about -50%. In the case with infinite resistance of the joints (*Model 2*), it is evaluated a  $T_R = 20$  years of activation that correspond to a decrease in term of  $I_R$  of about -45% than those reported in **Table 7** for  $KL=1$ .

The I.D.A. results are reported in **Figures 14b-15b** by dashed lines for lumped plasticity and continuous lines for diffused plasticity. Concerning diffuse plasticity, it observes homogeneous structural response by varying the modelling and the seismic input at the base, as the capacity curves are very close during both elastic and plastic phases. Differently, for lumped plasticity it observes a major dispersion on IDA capacity curves. Finally, a dashed vertical line is reported in the **Figures 14b-15b** in correspondence to the triggered mechanism in the dowel pins. It is the same point of lumped plasticity in **Sect. 4.3**, i.e. a scaled T.H. of a 0.2 factor, that corresponds to an average PGA 0.065g associated to a recurrence period  $T_R$  of 15 years ( $I_R=0.243$ ).

## 6 Conclusions

The seismic vulnerability assessment of industrial PS erected in Italy among the end of the 1960s and of the 1970s has been investigated. Elastic, nonlinear static and nonlinear dynamic analyses have been performed on a representative building. The choice was based on a large investigation on structural typologies, details and materials. Lumped and diffuse plasticity models have been used to compare the results in terms of global response and Seismic Risk Index ( $I_R$ ).

Linear dynamics and nonlinear static analyses, performed according to EC8 [25] and NTC2008 [20], suggest that:

1. a primary role is played by connections between elements, which are the critical aspect for the seismic upgrade of existing precast RC structures;
2. the mechanical slenderness of the columns can influence the overall response of the buildings but only when the connections are upgraded;

3. to reach a normal or full knowledge level, i.e. KL2 or KL3, no matter the resistance of the materials, does not involve some advantages in terms of  $I_R$  when the connections are modelled with the actual stiffness;
4. in all the cases, excluding “a priori” the possibility of the concrete spalling gives a sensible error in the evaluated seismic action;
5. the diffused and lumped plasticity models give acceptable results if the pushover analysis is done, and very good results if the I.D.A. is performed.

Nonlinear dynamic analysis, performed on space models subjected to ten different earthquakes, confirm that the capacity in terms of column chord rotation is not the critical aspect. This confirms observations of real events even if it notices a connection with limited resistance. This circumstance is much more relevant whenever existing structures are considered. Careful design of new precast systems and components can mitigate, however, such phenomena.

## REFERENCES

- [1] A.S. Elnashai, L. Di Sarno, Fundamentals of Earthquake Engineering, 2008. doi:10.1002/9780470024867.fmatter/pdf.
- [2] L. Liberatore, L. Sorrentino, D. Liberatore, L.D. Decanini, Failure of industrial structures induced by the Emilia (Italy) 2012 earthquakes, *Eng. Fail. Anal.* 34 (2013) 629–647. doi:10.1016/j.engfailanal.2013.02.009.
- [3] E. Artioli, R. Battaglia, A. Tralli, Effects of May 2012 Emilia earthquake on industrial buildings of early '900 on the Po river line, *Eng. Struct.* 56 (2013) 1220–1233. doi:10.1016/j.engstruct.2013.06.026.
- [4] M. Ercolino, G. Magliulo, G. Manfredi, Failure of a precast RC building due to Emilia-Romagna earthquakes, *Eng. Struct.* 118 (2016) 262–273. doi:10.1016/j.engstruct.2016.03.054.
- [5] M. Saatcioglu, D. Mitchell, R. Tinawi, N.J. Gardner, A.G. Gillies, A. Ghobarah, et al., The August 17, 1999, Kocaeli (Turkey) earthquake; damage to structures, *Can. J. Civ. Eng.* 28 (2001) 715–737. doi:10.1139/I01-043.
- [6] L. Tzenov, Sotirov, P. Boncheva, Study of some damaged industrial buildings due to Vrancea earthquake, in: 6th ECEE Dubrovnik, 1978: pp. 59–65.
- [7] P. Fajfar, J. Duhovnik, J. Reflak, M. Fishinger, Z. Breska, The behaviour of Buildings and other structures during the earthquake of 1979 in Montenegro, *Univ. Ljubljana, IKPIR Publ. No 19A.* (1981).
- [8] EERI, Armenia earthquake reconnaissance report, *Earthq. Spectra Suppl.* (1989).
- [9] G. Bonacina, M. Indirli, P. Negro, The January 17, 1994 Northridge Earthquake—report to the sponsor: earthquake engineering field investigation team, *Spec. Publ. No. I.94.14.* (1994).
- [10] G. Magliulo, V. Capozzi, G. Fabbrocino, G. Manfredi, Neoprene–concrete friction relationships for seismic assessment of existing precast buildings, *Eng. Struct.* 33 (2011) 532–538. doi:10.1016/j.engstruct.2010.11.011.
- [11] G. Magliulo, G. Fabbrocino, G. Manfredi, Seismic assessment of existing precast industrial buildings using static and dynamic nonlinear analyses, *Eng. Struct.* 30 (2008) 2580–2588. doi:10.1016/j.engstruct.2008.02.003.
- [12] B. Zoubek, T. Isakovic, Y. Fahjan, M. Fischinger, Cyclic failure analysis of the beam-to-column dowel connections in precast industrial buildings, *Eng. Struct.* 52 (2013) 179–191. doi:10.1016/j.engstruct.2013.02.028.
- [13] D. Asprone, R. De Risi, G. Manfredi, Defining structural robustness under seismic and simultaneous



actions: an application to precast RC buildings, *Bull. Earthq. Eng.* 14 (2016) 485–499.  
doi:10.1007/s10518-015-9820-4.

- [14] P. Negro, E. Mola, L. Ferrara, B. Zhao, G. Magonette, J. Molina, PRECAST EC8: seismic behaviour of precast concrete structures with respect to Eurocode 8. Final Report of the experimental activity of the Italo-Slovenian Group, Parts 1, 2, 3, FP6 Project No. G6RD-CT-2002-00857, 2007.
- [15] M.H. Carydis PG, Psycharis IN, PRECAST EC8: Seismic Behaviour of precast concrete structures with respect to Eurocode 8. Final Report of the contribution of LEE/NTUA, FP5 Project No. G6RD-CT-2002-00857, 2007.
- [16] I.N. Psycharis, H.P. Mouzakis, Shear resistance of pinned connections of precast members to monotonic and cyclic loading, *Eng. Struct.* 41 (2012) 413–427. doi:10.1016/j.engstruct.2012.03.051.
- [17] G.D. Kremmyda, Y.M. Fahjan, S.G. Tsoukantas, Nonlinear FE analysis of precast RC pinned beam-to-column connections under monotonic and cyclic shear loading, *Bull. Earthq. Eng.* 12 (2014) 1615–1638. doi:10.1007/s10518-013-9560-2.
- [18] G. Magliulo, M. Ercolino, M. Cimmino, V. Capozzi, G. Manfredi, FEM analysis of the strength of RC beam-to-column dowel connections under monotonic actions, *Constr. Build. Mater.* 69 (2014) 271–284. doi:10.1016/j.conbuildmat.2014.07.036.
- [19] P. Negro, D. a. Bournas, F.J. Molina, Pseudodynamic tests on a full-scale 3-storey precast concrete building: Global response, *Eng. Struct.* 57 (2013) 594–608. doi:10.1016/j.engstruct.2013.05.047.
- [20] NTC2008, Decreto Ministeriale del 14.1.2008. Nuove Norme Tecniche per le Costruzioni. (in Italian), (2008).
- [21] Circolare Ministeriale n. 617, Cons. Sup. LL. PP., 'Istruzioni per l'applicazione delle Nuove Norme Tecniche per le Costruzioni' di cui al decreto ministeriale del 14.01.2008. G.U. del 26.02.2009 n. 47, supplemento ordinario n. 27. (in Italian), (2009).
- [22] JBDPA, Standard for seismic capacity evaluation of existing reinforced concrete buildings, (1977).
- [23] FEMA, Earthquake Loss Estimation Methodology, (1999).
- [24] Reluis, P. Civile, Interventi locali e globali su edifici industriali monopiano non progettati con criteri antisismici (in Italian), (2012).
- [25] CEN (Comité Européen de Normalisation), Eurocode 8: Design of structures for earthquake resistance – Part 1: General rules, seismic actions and rules for buildings (EN 1998-1), (2004).
- [26] International Federation for Structural Concrete—fib, Structural connections for precast concrete buildings - Bullettin n. 43, Lausanne, 2008.
- [27] International Federation for Structural Concrete—fib, Seismic design of precast concrete build - Bullettin no. 27, Lausanne, 2003.
- [28] G. Magliulo, M. Ercolino, C. Petrone, O. Coppola, G. Manfredi, The Emilia Earthquake: Seismic Performance of Precast Reinforced Concrete Buildings, *Earthq. Spectra.* 30 (2014) 891–912. doi:10.1193/091012EQS285M.
- [29] F. Saitta, G. Bongiovanni, G. Buffarini, P. Clemente, A. Martelli, A. Marzo, et al., Behaviour of industrial buildings in the Pianura Padana Emiliana Earthquake, *EAI - Energia, Ambient. E Innov.* 4-5/Part I (2012) 47–57. <http://www.enea.it/it/pubblicazioni/pdf-eai/luglio-ottobre-2012/seconda-parte/behaviour-industrial-buildings-pdf>.
- [30] C. Casotto, V. Silva, H. Crowley, R. Nascimbene, R. Pinho, Seismic fragility of Italian RC precast industrial structures, *Eng. Struct.* 94 (2015) 122–136. doi:10.1016/j.engstruct.2015.02.034.
- [31] A. Belleri, E. Brunesi, R. Nascimbene, M. Pagani, P. Riva, Seismic Performance of Precast Industrial Facilities Following Major Earthquakes in the Italian Territory, *J. Perform. Constr. Facil.* 29 (2015) 04014135. doi:10.1061/(ASCE)CF.1943-5509.0000617.
- [32] CNR, Istruzioni per il progetto, l'esecuzione e il controllo delle strutture prefabbricate in conglomerato cementizio e per le strutture costruite con sistemi industrializzati - CNR 10025/84 (in Italian), (1985) 166.



- [33] CNR, Istruzioni per il progetto, l'esecuzione ed il controllo delle strutture prefabbricate in calcestruzzo - CNR 10025/98 (in Italian), (2000).
- [34] CEN (Comité Européen de Normalisation), Eurocode 8 - Design of structures for earthquake resistance - Part 3: Assessment and retrofitting of buildings - EN 1998-3, (2005).
- [35] F. Clementi, E. Quagliarini, G. Maracchini, S. Lenci, Post-World War II Italian school buildings: typical and specific seismic vulnerabilities, *J. Build. Eng.* 4 (2015) 152–166. doi:10.1016/j.job.2015.09.008.
- [36] Law 25 November 1962 (n. 1684). Provvedimenti per l'edilizia, con particolari prescrizioni per le zone sismiche (in Italian). (GU n.326 del 22-12-1962 - Suppl. Ordinario ), (1962).
- [37] Law 5 November 1964 (n. 1224). Integrazioni della legge 25 novembre 1962 n. 1684, concernente provvedimenti per l'edilizia con particolari prescrizioni per le zone sismiche (in Italian). (GU n.297 del 1-12-1964 ), (1964).
- [38] Circ. M. LL. PP. n. 1422 - 6 February 1965. Istruzioni per il rilascio della dichiarazione di idoneità tecnica dei sistemi costruttivi e strutture portanti prevista negli art. 1 e 2 della Legge 5 novembre 1964, n. 1244 con particolare riferimento alle str, (1965).
- [39] D. M. 3/12/1987. Norme tecniche per la progettazione, esecuzione e collaudo delle costruzioni prefabbricate. G.U. n. 106 del 7/5/1988 (in Italian)., (1987).
- [40] Ordinanza del Presidente del Consiglio dei Ministri (OPCM). General criteria for the seismic classification of the national territory and technical standards for constructing in seismic zones. Ordinance no. 3274, G.U. n. 72 del 8–5-2003 (in Italian), (2003).
- [41] B. Højlund-Rasmussen, Betoninstøbte, tvaerbelastade boltes og dornes bæreevne. (Resistance of embedded bolts and dowels loaded in shear. In Danish), *Bygningsstatiske Meddelelser*. 34 (1963).
- [42] T.P. Tassios, E.N. Vintzēleou, Mathematical models for dowel action under monotonic and cyclic conditions, *Mag. Concr. Res.* 38 (1986) 13–22. doi:10.1680/mac.1986.38.134.13.
- [43] E. N. Vintzeleou and T. P. Tassios, Behavior of Dowels Under Cyclic Deformations, *ACI Struct. J.* 84 (1987) 13. doi:10.14359/2749.
- [44] B. Engström, Combined effects of dowel action and friction in bolted connections, *Nord. Concr. Res.* 9 (1990) 14–33.
- [45] J. Walvaren, Model Code 2010, final drafts, *FIB Bull.* 1 & 2 (2012) 105.
- [46] P. Soroushian, K. Obaseki, M. Rojas, J. Sim, Analysis of Dowel Bars Acting Against Concrete Core, *ACI J. Proc.* 83 (1986) 642–649. doi:10.14359/10657.
- [47] P. Soroushian, K. Obaseki, M. Rojas, H.S. Najm, Behavior of Bars in Dowel Action Against Concrete Cover, *ACI Struct. J.* 84 (1987) 170–176. doi:10.14359/2847.
- [48] P. Negro, G. Toniolo, Design Guidelines for Connections of Precast Structures under Seismic Actions Third Main Title Line Third Line, 2012. doi:10.2777/37605.
- [49] SAFECast. Performance of innovative mechanical connections in precast building structures under seismic conditions, (2009).
- [50] A. Belleri, M. Torquati, P. Riva, R. Nascimbene, Vulnerability assessment and retrofit solutions of precast industrial structures, *Earthquakes Struct.* 8 (2015) 801–820. doi:10.12989/eas.2015.8.3.801.
- [51] Midas GEN, Analysis Manual, (2015).
- [52] A. Pierdicca, F. Clementi, M. Maracci, D. Isidori, S. Lenci, Vibration-Based SHM of Ordinary Buildings: Detection and Quantification of Structural Damage, in: *ASME Proceedings (Ed.)*, ASME 2015 Int. Des. Eng. Tech. Conf. Comput. Inf. Eng. Conf., Boston, Massachusetts, USA, 2015: p. 8. doi:10.1115/DETC2015-46763.
- [53] E. Vanmarcke, E. H., Fenton, G. A., Heredia-Zavoni, SIMQKE-II: Conditioned Earthquake Ground Motion Simulator, (2011).
- [54] I. Iervolino, C. Galasso, E. Cosenza, REXEL: computer aided record selection for code-based seismic structural analysis, *Bull. Earthq. Eng.* 8 (2010) 339–362. doi:10.1007/s10518-009-9146-1.

- [55] Presidenza del Consiglio dei Ministri, OPCM 3728/08 (in Italian), (2008).
- [56] P. Fajfar, P. Gašperšič, The N2 method for the seismic damage analysis of rc buildings, *Earthq. Eng. Struct. Dyn.* 25 (1996) 31–46. doi:10.1002/(SICI)1096-9845(199601)25:1<31::AID-EQE534>3.0.CO;2-V.
- [57] G. Magliulo, G. Maddaloni, E. Cosenza, Comparison between non-linear dynamic analysis performed according to EC8 and elastic and non-linear static analyses, *Eng. Struct.* 29 (2007) 2893–2900. doi:10.1016/j.engstruct.2007.01.027.
- [58] CEN (Comité Européen de Normalisation), Eurocode 2 - Design of concrete structures Part 1-1: General rules and rules for buildings - EN 1992-1-1, (2005).
- [59] D. Vamvatsikos, C.A. Cornell, Incremental dynamic analysis, *Earthq. Eng. Struct. Dyn.* 31 (2002) 491–514. doi:10.1002/eqe.141.
- [60] T. Takeda, M. a. Sozen, N.N. Nielsen, Reinforced Concrete Response to Simulated Earthquakes, *J. Struct. Div.* 96 (1970) 2557–2573. <http://cedb.asce.org/cgi/WWWdisplay.cgi?17038>.
- [61] E. Spacone, F.C. Filippou, F.F. Taucer, Fibre beam-column model for non-linear analysis of r/c frames: part i. formulation, *Earthq. Eng. Struct. Dyn.* 25 (1996) 711–725. doi:10.1002/(SICI)1096-9845(199607)25:7<711::AID-EQE576>3.0.CO;2-9.
- [62] D.C. Kent, R. Park, Flexural members with confined concrete, *J. Struct. Div.* 97 (1971) 1969–1990.
- [63] M., Menegotto, P.E., Pinto, Method of anaysis for cyclically loaded reinforced concrete plane frames including changes in geometry and non-elastic behavior of elements under combined normal force and bending, in: I.A. of B. and S. Engineering (Ed.), IABSE Symp. Resist. Ultim. Deform. Struct. Acted by WellDefined Repeated Loads, Lisbon, 1973.

## **HIGHLIGHTS**

- A relevant case study was recognized inside a large scale of seismic vulnerability assessment of these types of structures.
- New specific seismic vulnerability was identified for this building typology .
- A sensitivity analyses have been carried out to assess the influences of dowel pin connections in r.c. precast buildings.
- The effective influence of these vulnerabilities on its seismic behaviour was quantified.
- The knowledge of these outcomes may help professional engineers and architects in designing suitable interventions in Europe.

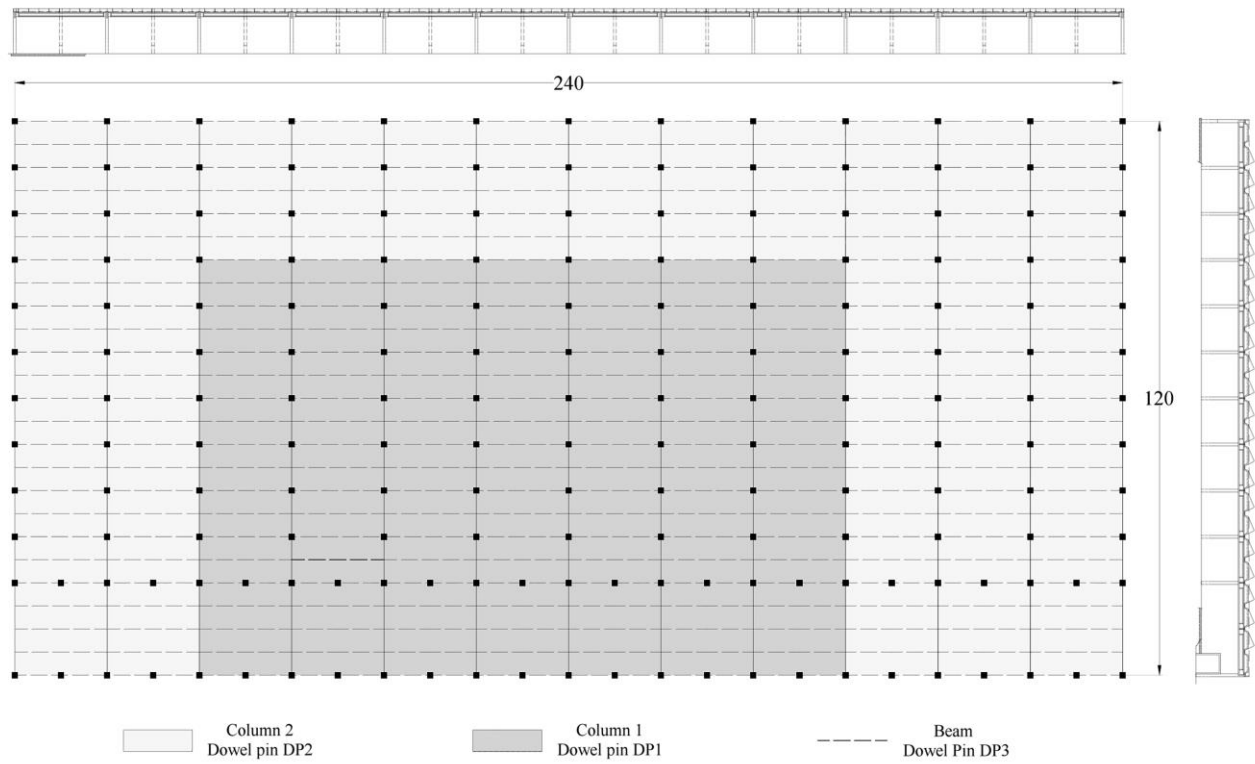


**Figure 1.** Geometry of the industrial building.

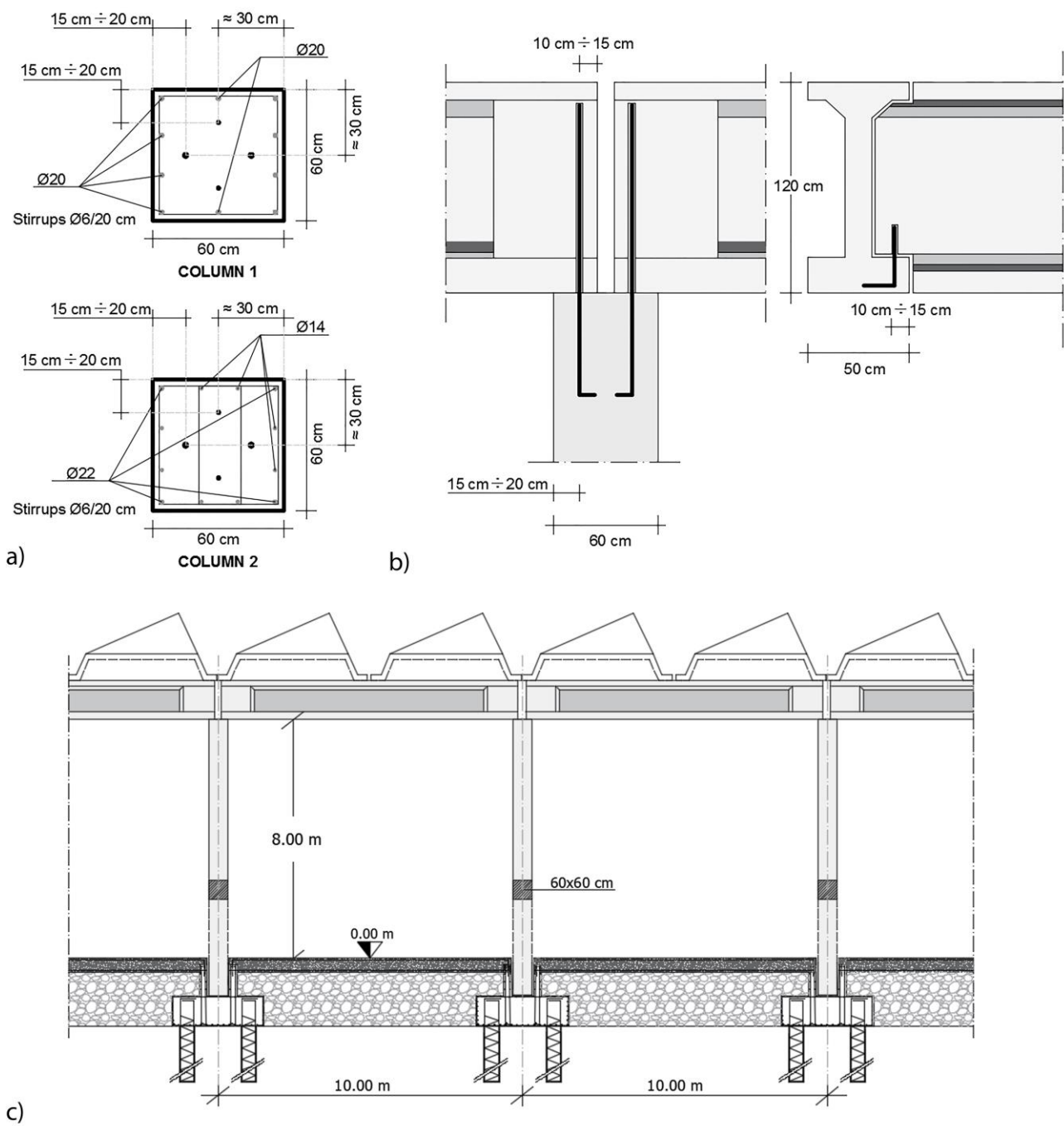


**Figure 2.** a) Main dimensions of the columns in the central part of the building, b) the dowel pin connections between columns-beams (Dowel pin 1 and 2) and beam-beam (Dowel pin 3), c) transversal section of the building.

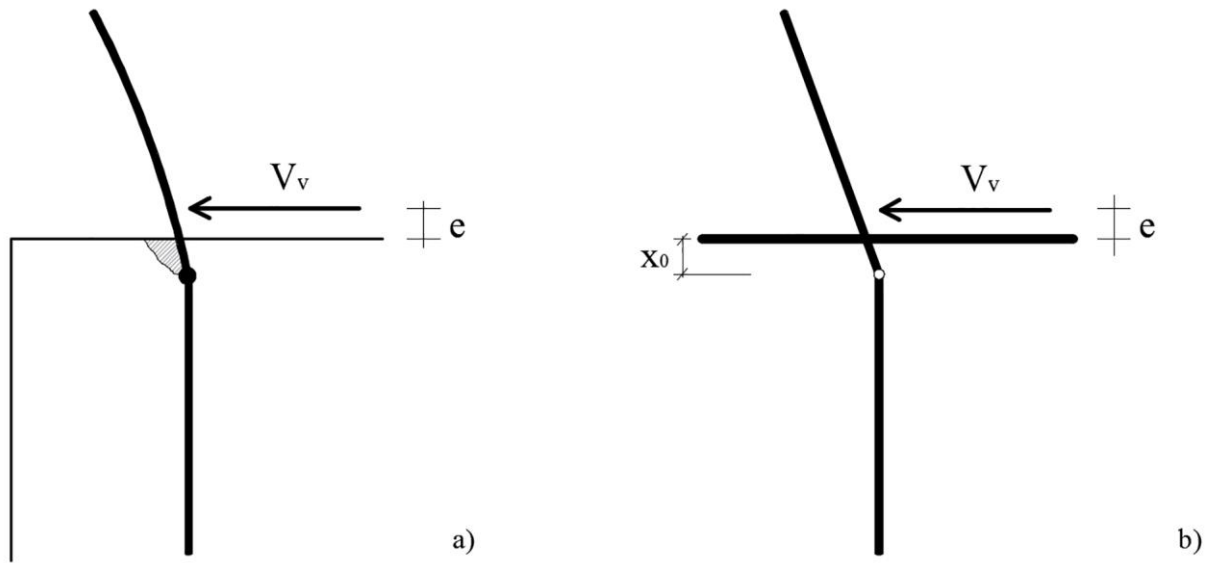


**Figure 3.** a) Splitting effects around dowel pin loaded in shear, b) Steel flexural failure with formation of a plastic hinge and settlement of the one-sided dowel pin in concrete that crushes locally under the high compressive stress.

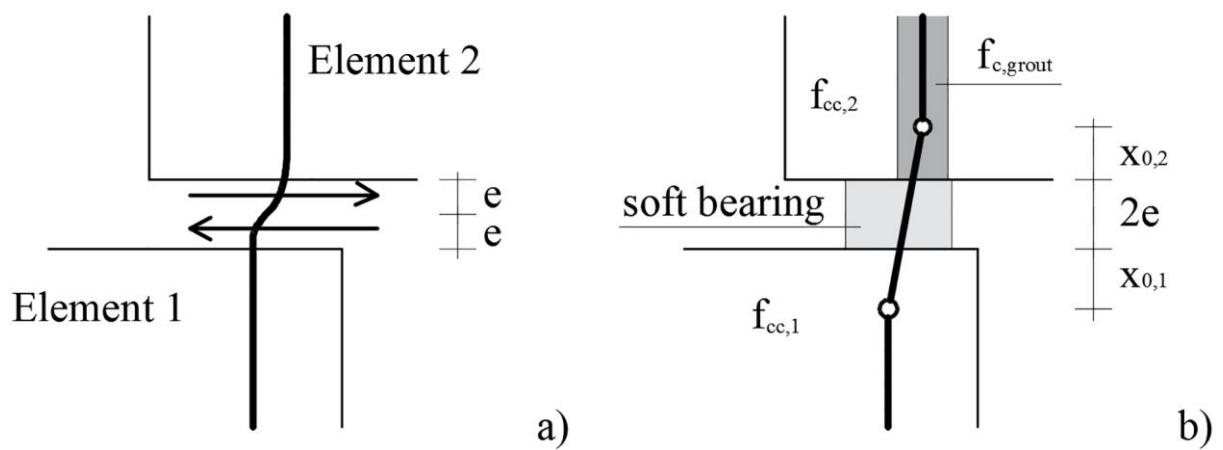


**Figure 4.** a) Shear transfer by dowel action in dowel pin with double fixation, b) double-sided plain dowel pin across a joint of a certain width and dowel action non-symmetrical condition.

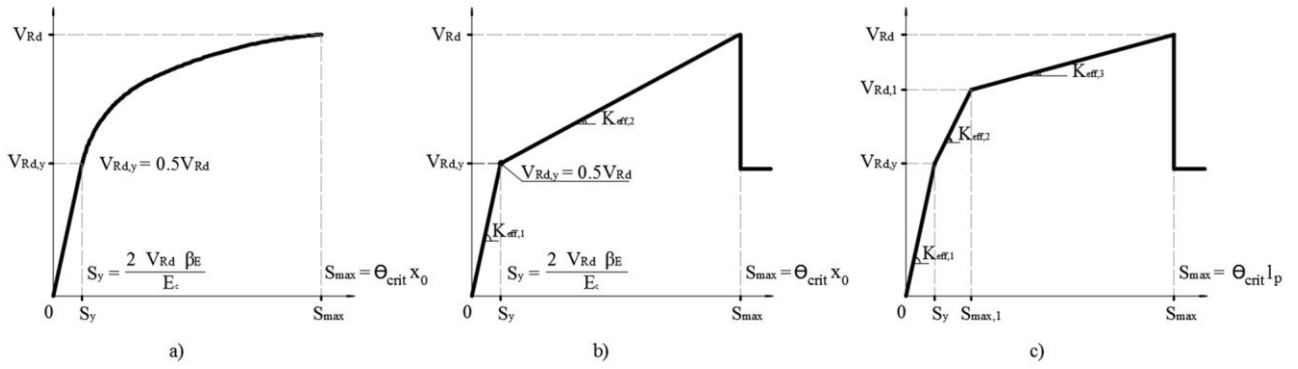


**Figure 5.** Nonlinear behaviour of dowel pin for steel flexural failure reported in Fib n. 43 [26] for: a) shear-displacement one-sided plain dowel, b) associated skeleton curve for one-sided dowel, c) tri-linear skeleton curve for double-sided connection with non-symmetrical conditions.





Figure 6. 3D view of the building model.

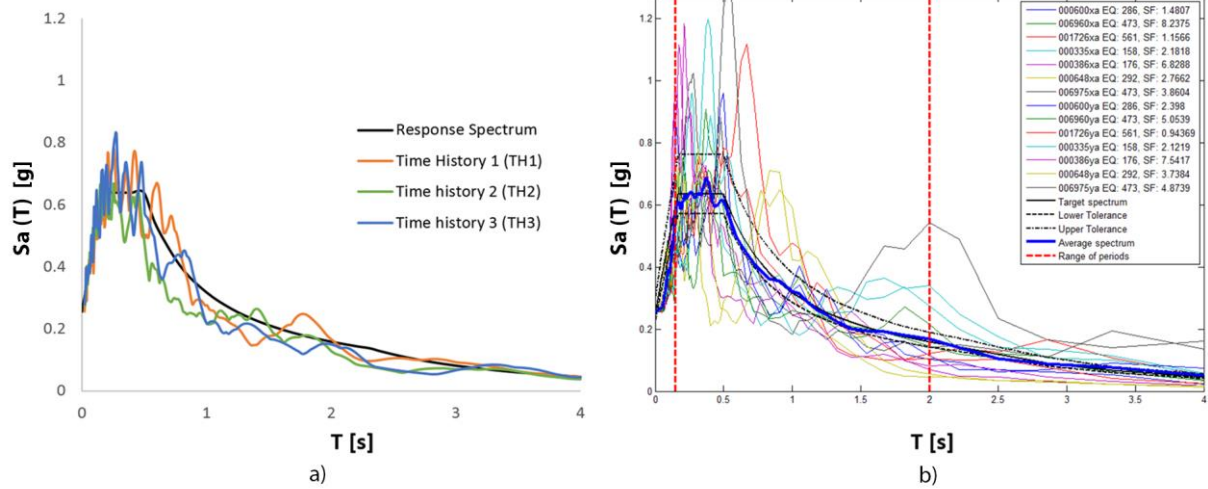
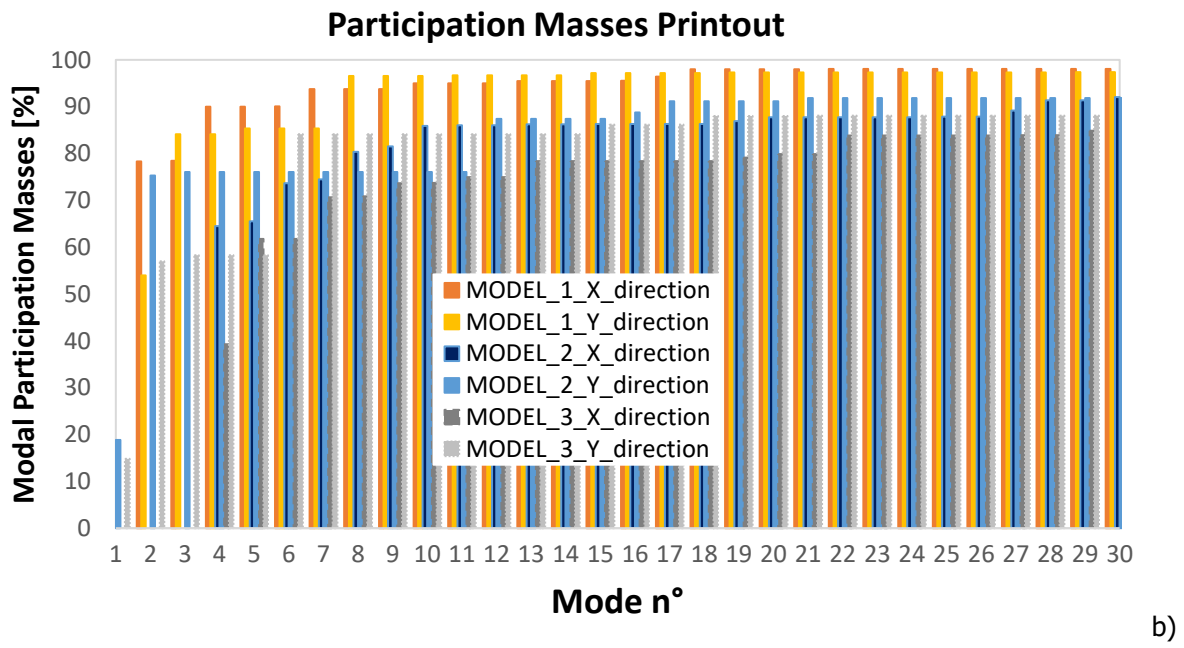
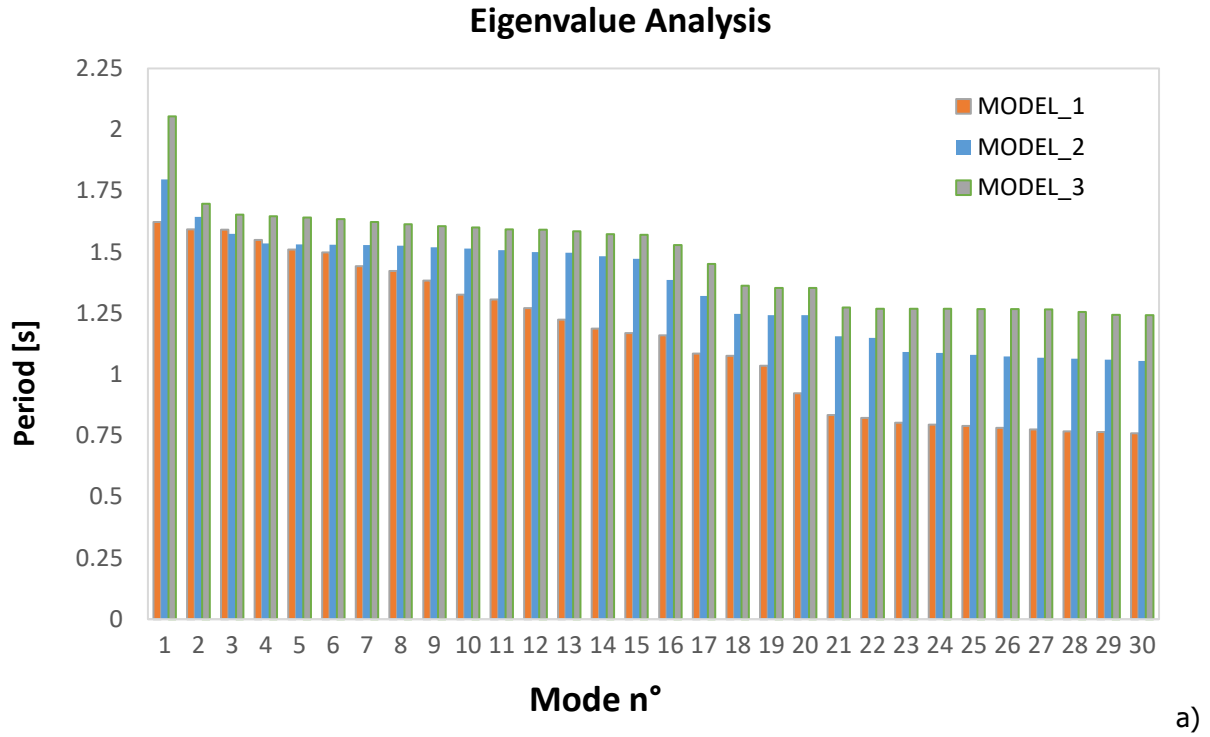
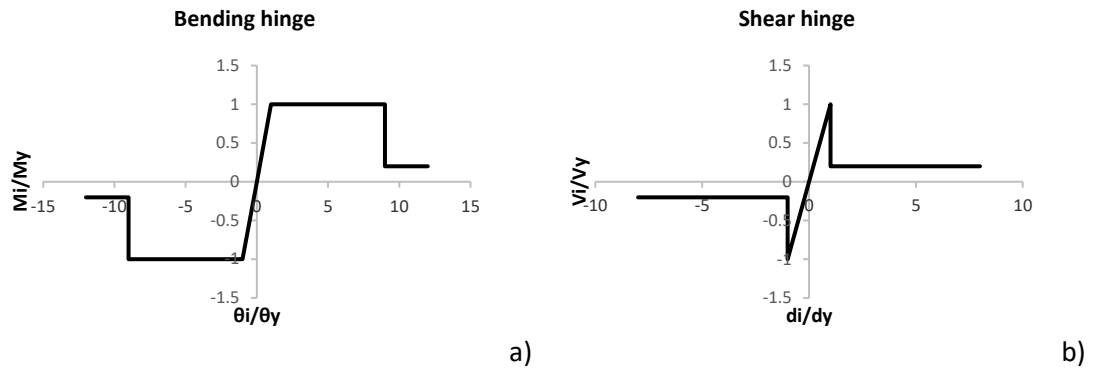


Figure 7. The reference response spectrum for  $T_{R,D}(SLSD)=475$  years and the spectra corresponding to the considered three (1-component) artificial ground accelerations (TH) spectrum compatible a), and seven (2-components) natural time histories spectrum compatible b), Damping  $\xi=5\%$ .



**Figure 8.** a) First 30 period, and b) the corresponding participation masses.



**Figure 9.** Non-dimensional force–deformation relationship adopted for: a) bending (only columns) and b) shear hinges (columns and general links for spalling rupture).

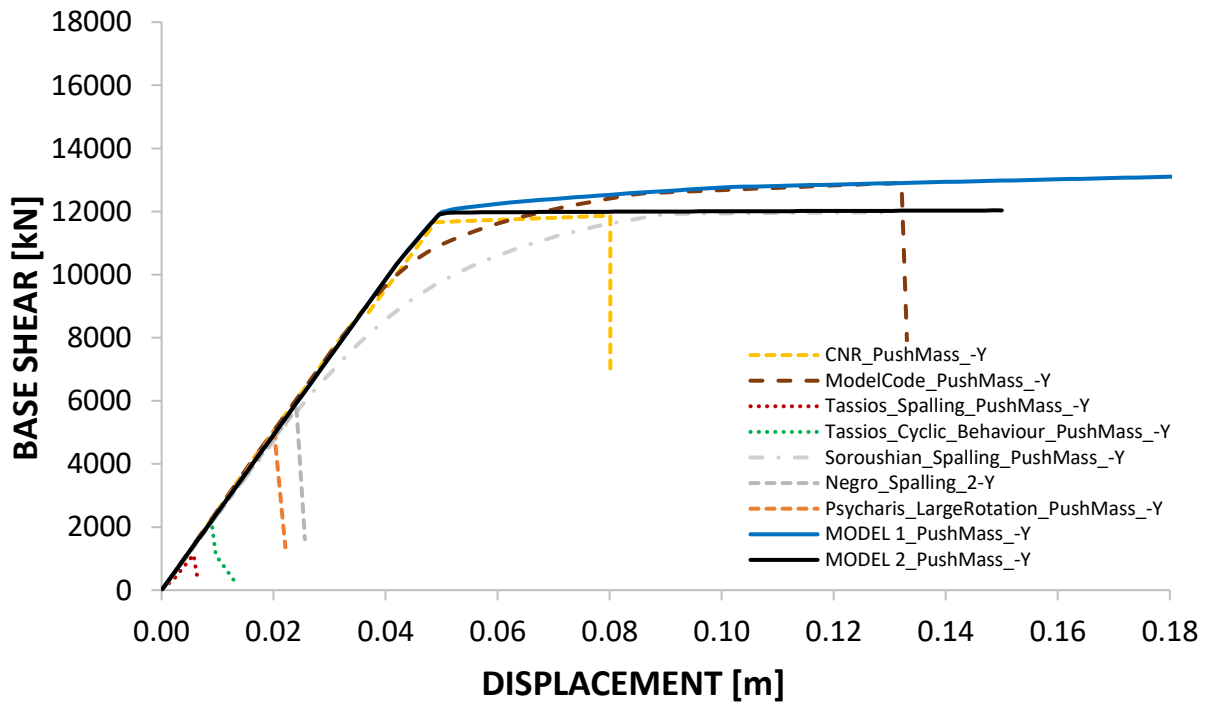
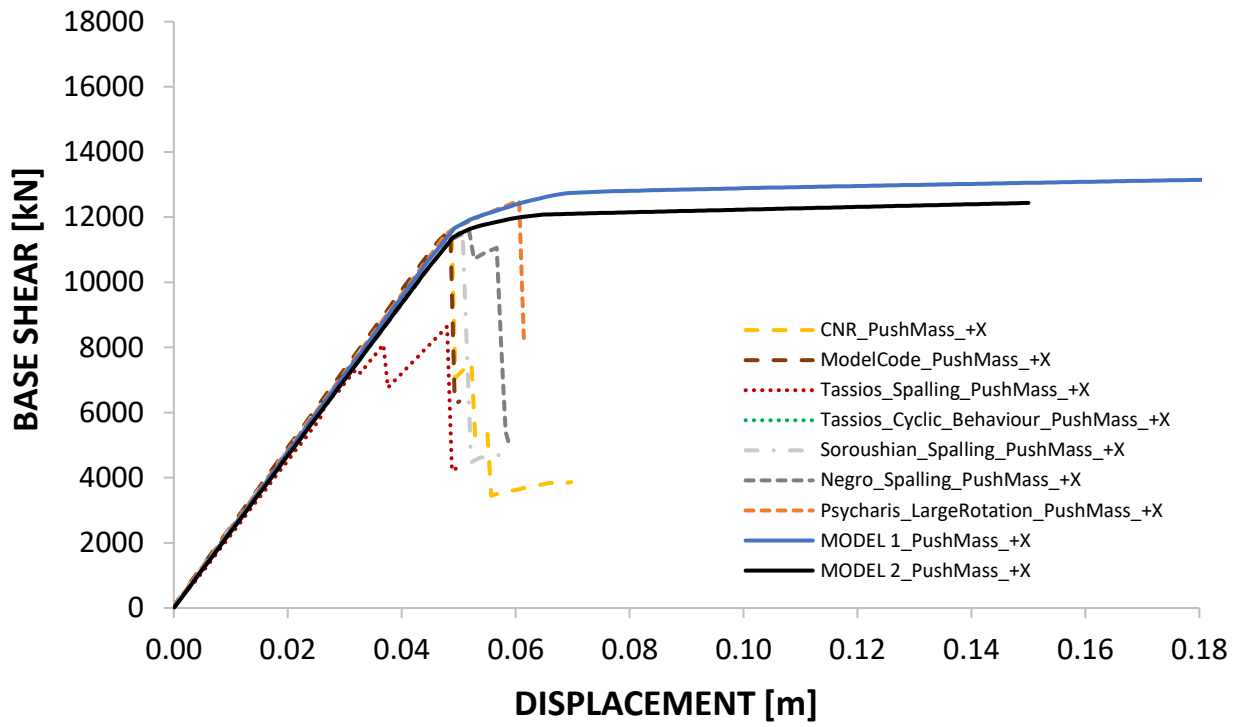
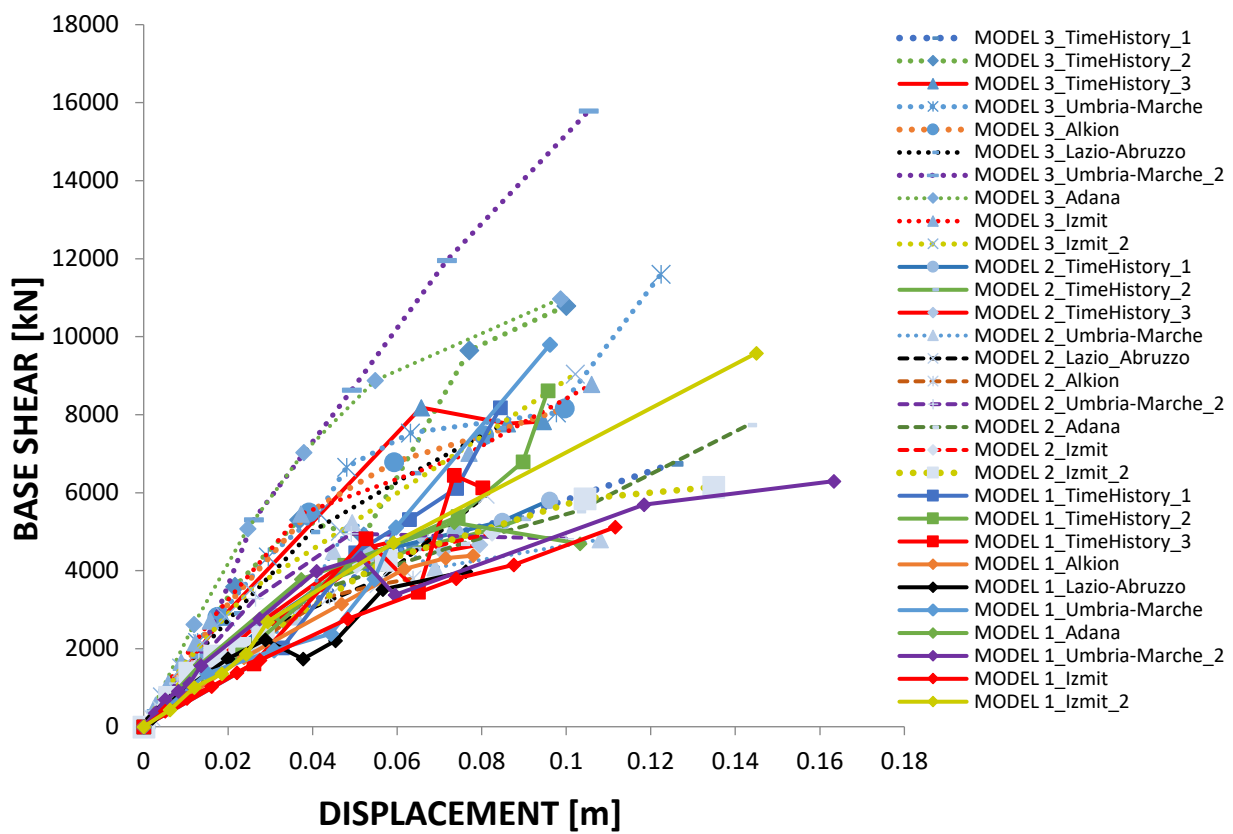
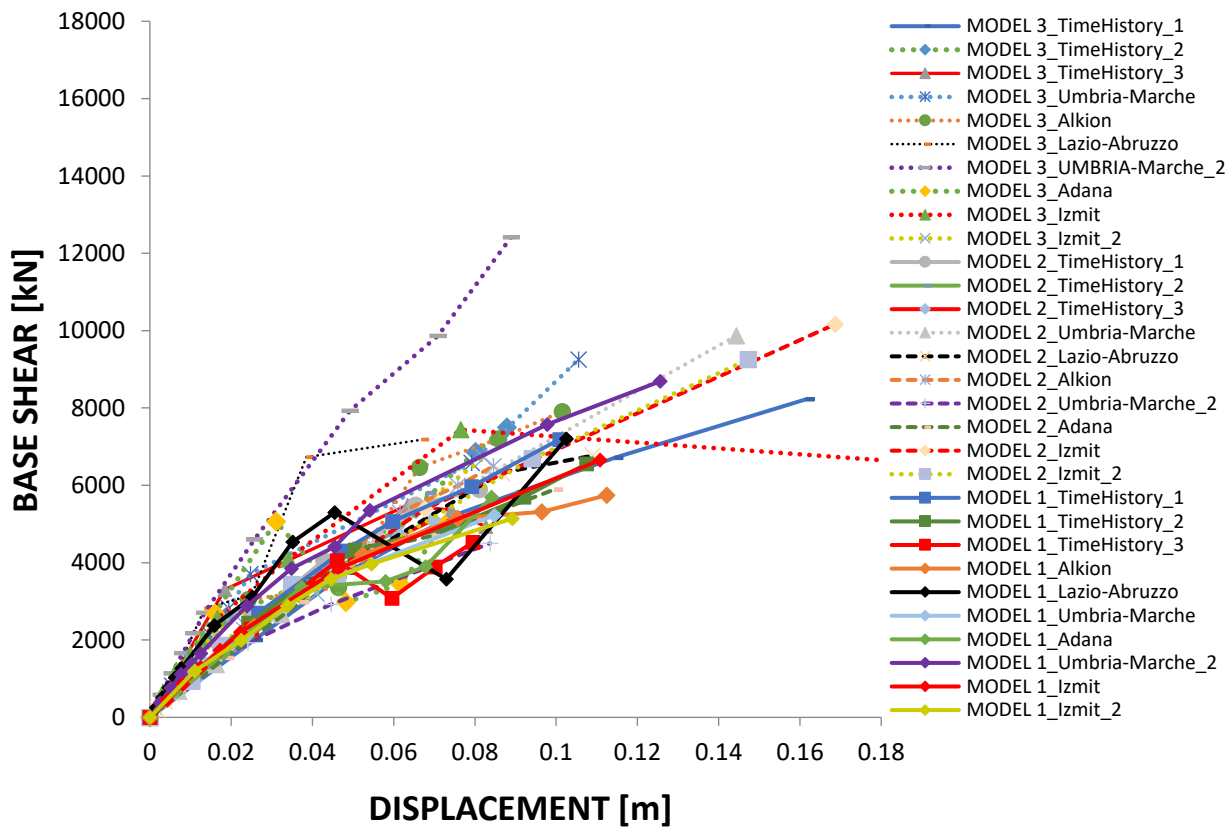


**Figure 10.** Comparison between capacity curves of different dowel pin capacity models (*Model 3*), cylindrical (*Model 1*) and spherical (*Model 2*) hinges models for PushMass distribution in: a) +X direction and, b) -Y direction.

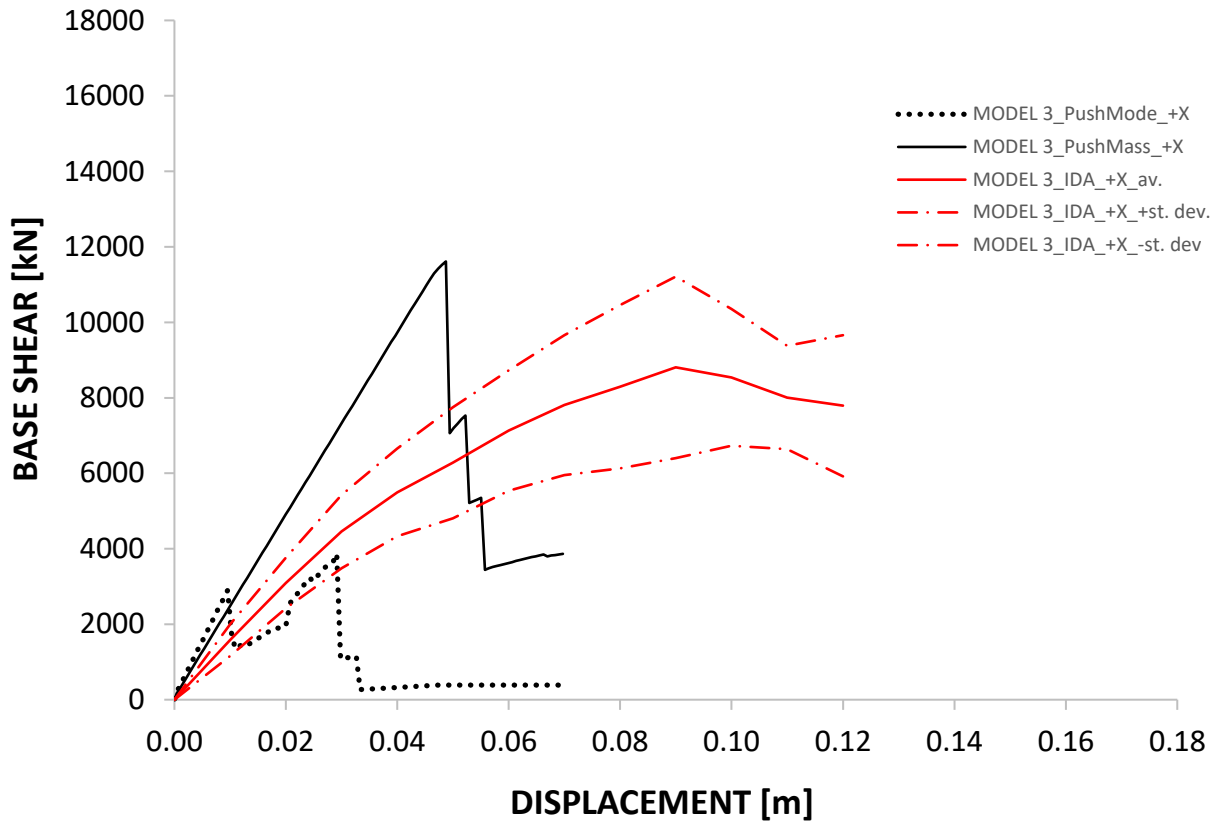


a)

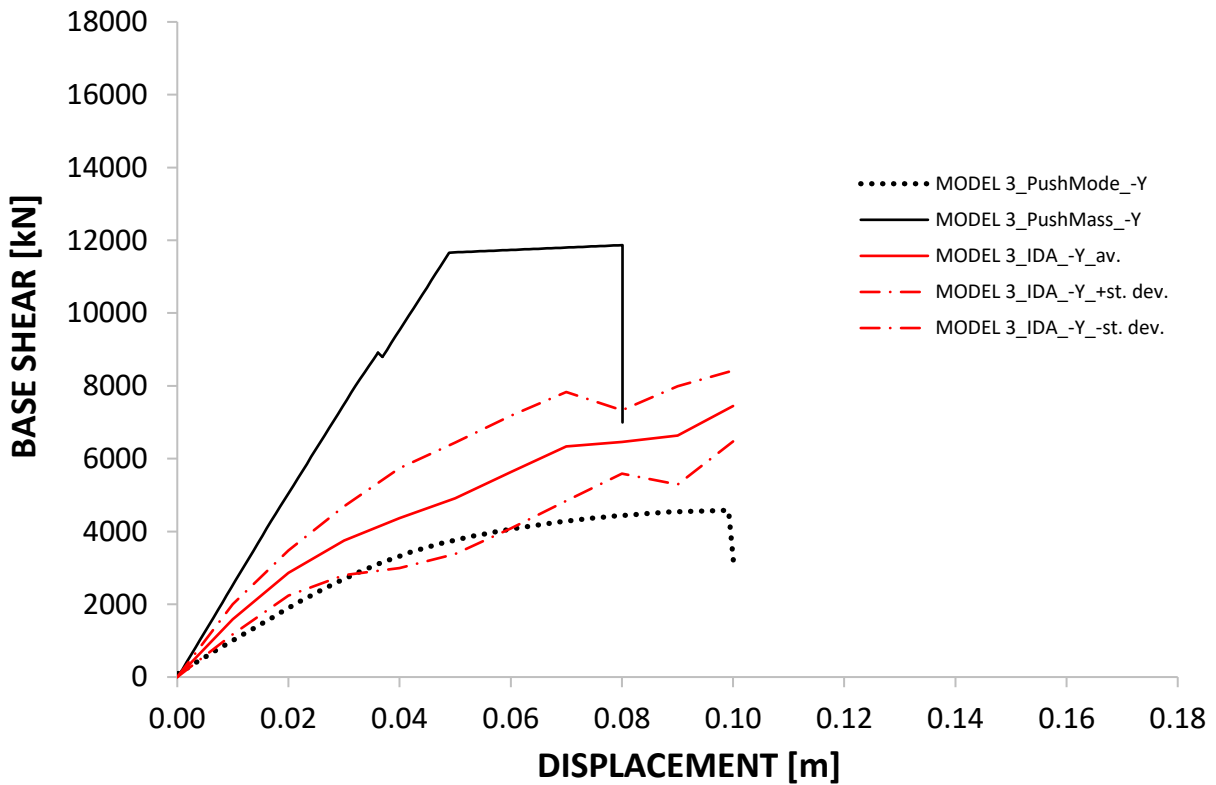


b)

Figure 11. I.D.A capacity curves for the ten time histories of the Model 1, 2 and 3: a) X-direction, b) Y-direction.

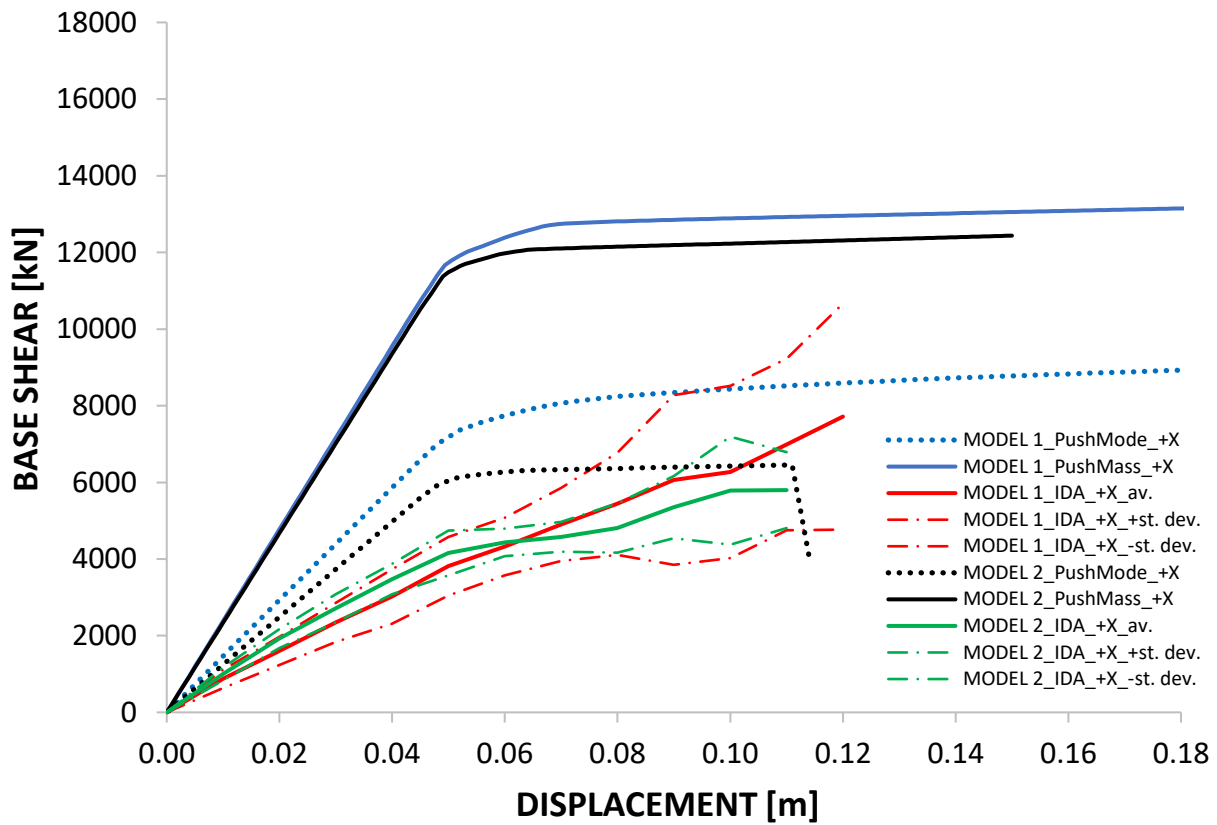


a)

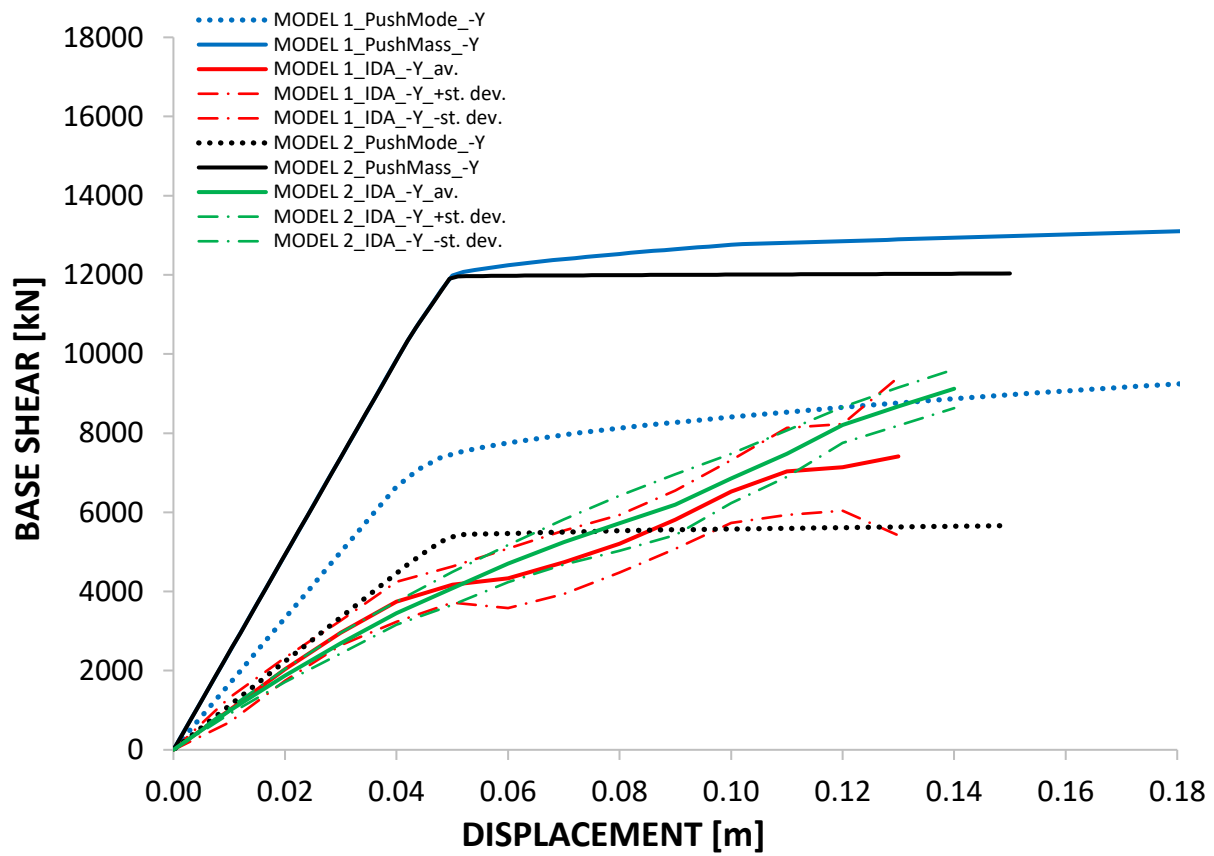


b)

**Figure 12.** Comparison between nonlinear static (both PushMode and PushMass distributions) and I.D.A. results for *Model 3* for: a) +X direction and, b) -Y direction.



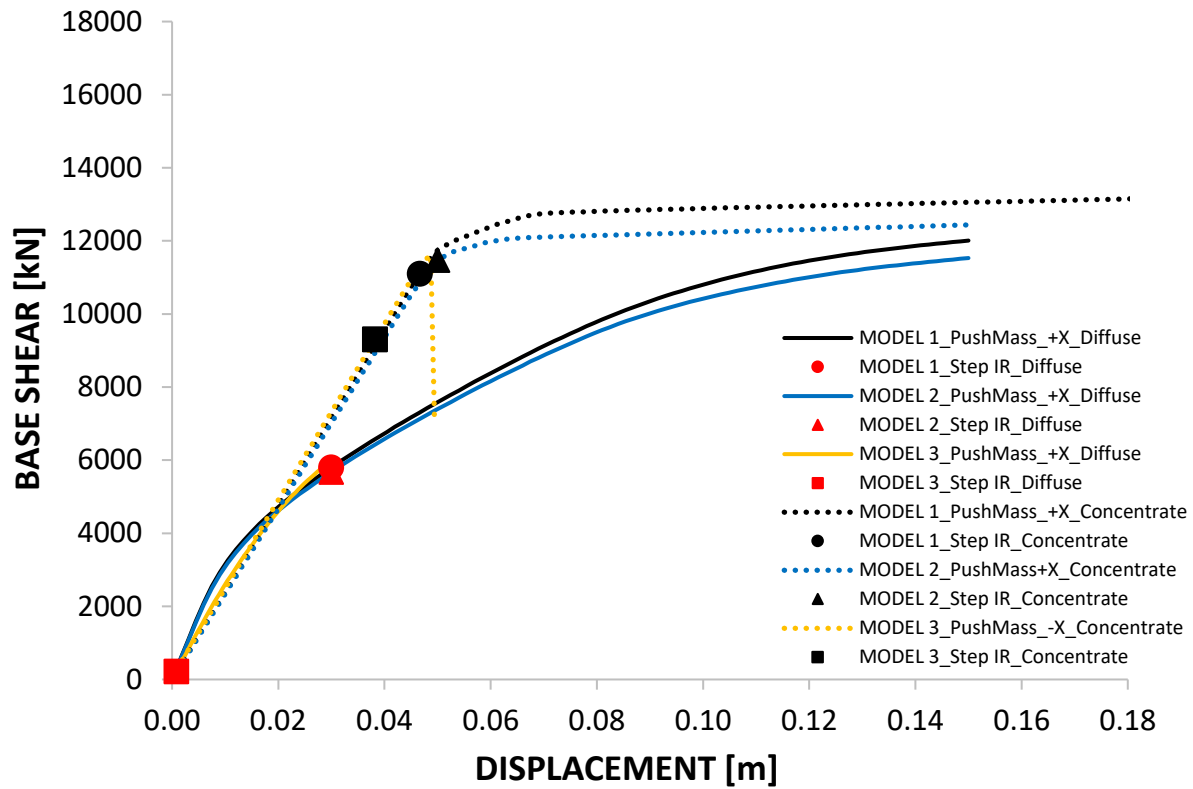
a)



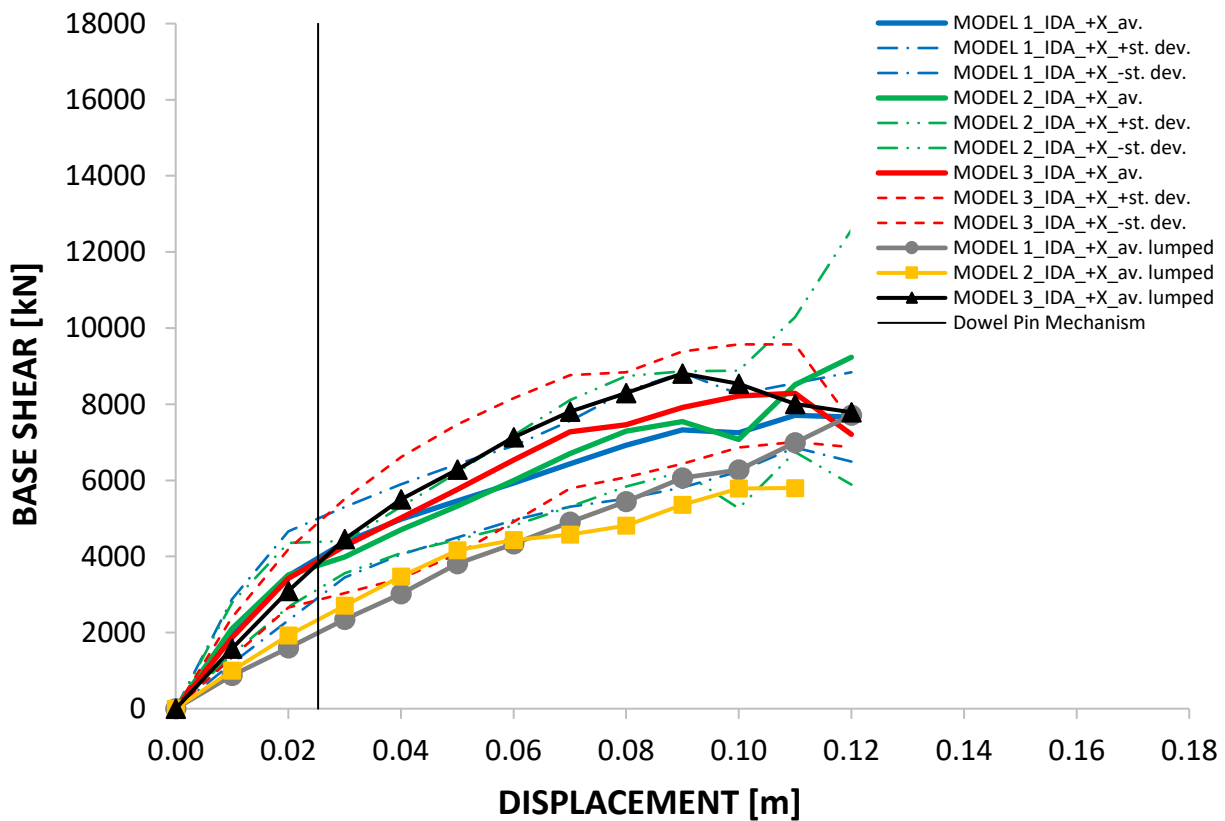
b)

**Figure 13.** Comparison between nonlinear static (both PushMode and PushMass distributions) and I.D.A. results for *Models 1 and 2* for: a) +X direction and, b) -Y direction.



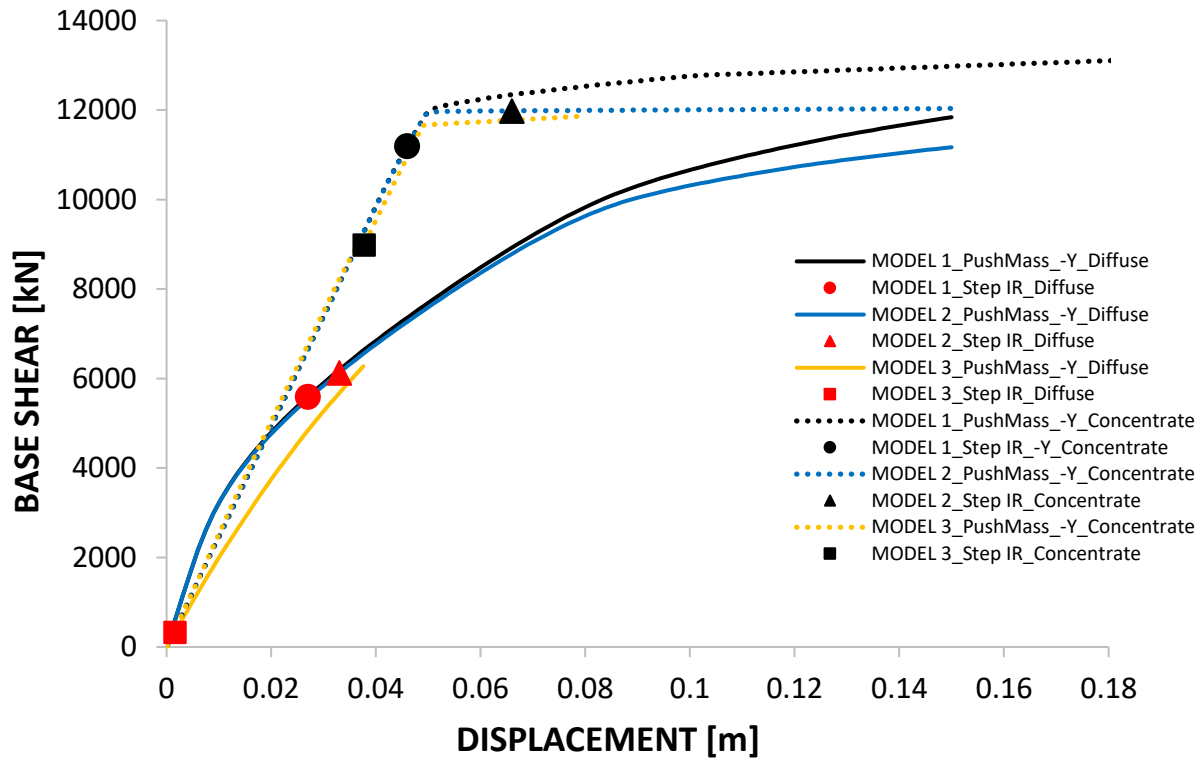


a)

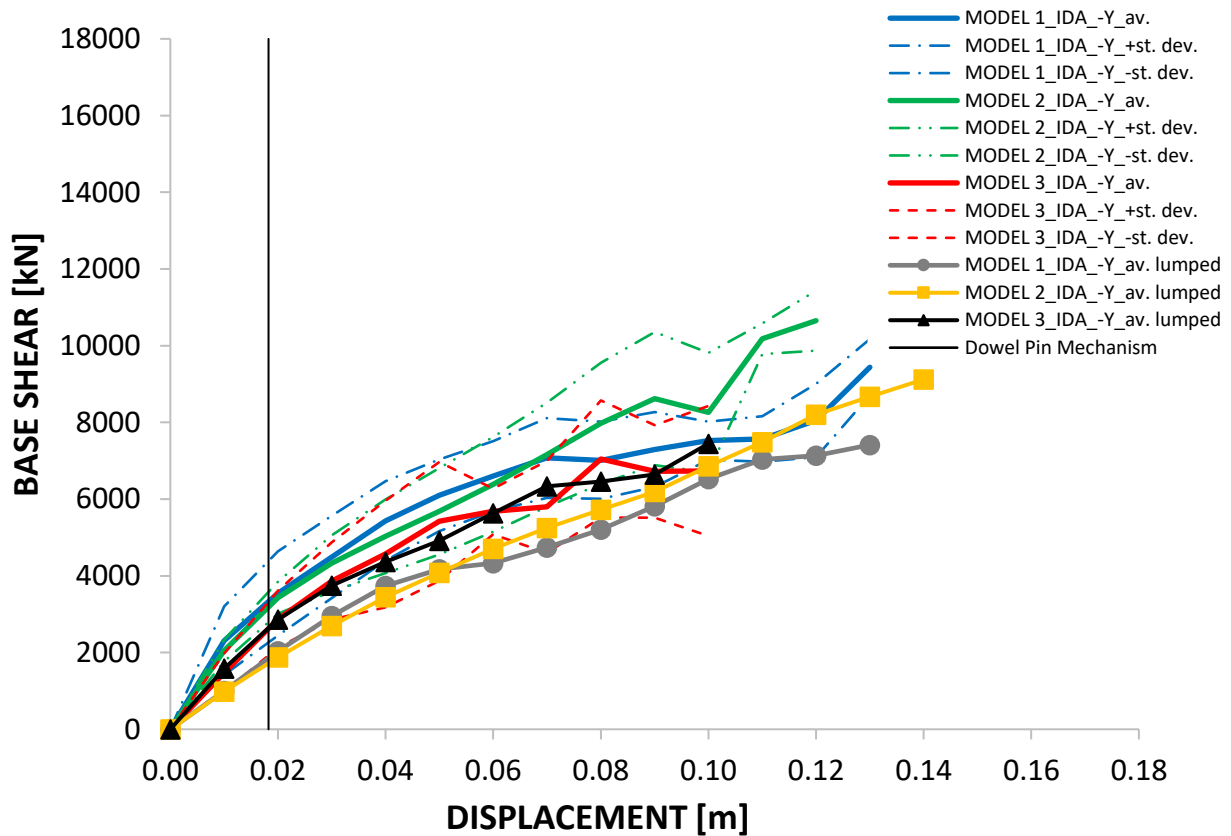


b)

**Figure 14.** Comparison between lumped (dashed line) and diffused plasticity (continuous line) in term of global response in +X direction for: a) nonlinear static analyses for PushMass distributions, and b) incremental dynamic analyses results with lumped (dotted lines) and diffused plasticity (continuous lines).



a)



b)

**Figure 15.** Comparison between lumped and diffused plasticity in term of global response in -Y direction for: a) nonlinear static analyses with lumped (dashed line) and diffused plasticity (continuous line) for PushMass distribution, b) incremental dynamic analyses results with lumped (dashed lines) and diffused plasticity (continuous lines).

	<b>f<sub>c</sub></b> <b>[MPa]</b>	<b>E<sub>m</sub></b> <b>[MPa]</b>	<b>f<sub>ym</sub> (bars/stirrups)</b> <b>[MPa]</b>	<b>Dowel</b> <b>Pin</b>
<b>Column 1</b>	30.0	22941.4	380/320	DP1
<b>Column 2</b>	35.3	24083.7	380/320	DP2
<b>Beam</b>	35.3	16055.8	380/320	DP3

**Table 1.** Mechanical characteristics of the main elements (see **Figure 1**), and relative dowel pin connection.

	<b>DOWEL PIN DP1</b> <b>V<sub>Rd</sub> [kN]</b>	<b>DOWEL PIN DP2</b> <b>V<sub>Rd</sub> [kN]</b>	<b>DOWEL PIN DP3</b> <b>V<sub>Rd</sub> [kN]</b>
<b>Fib Bulletin 43</b>	51.68	56.06	29.65
<b>CNR 10025/84</b>	62.01	67.27	35.58
<b>Tassios, Vintzeleou</b>			
<i>flexural failure (f.f.)</i>	67.18	72.87	38.54
<i>concrete spalling</i>	7.37	8.21	5.05
<i>cyclic behaviour (f.f.)</i>	33.59	36.44	19.27
<b>MODEL CODE 2010</b>	64.91	70.41	37.24
<b>Negro, Toniolo</b>			
<i>concrete spalling</i>	37.34	40.50	31.87
<b>Psycharis, Mouzakis</b>			
<i>small rotations (f.f.)</i>	56.84	61.66	32.61
<i>large rotations (f.f.)</i>	46.51	50.45	26.68
<b>Soroushian</b>			
<i>flexural failure</i>	48.43	49.65	27.4
<i>concrete spalling</i>	77.77	86.68	68.97

**Table 2.** Shear capacity V<sub>Rd</sub> [kN] of the three different dowel pin considered in the analyses.

<b>Waveform</b> <b>ID</b>	<b>Earthquake</b> <b>ID</b>	<b>Station</b> <b>ID</b>	<b>Earthquake</b> <b>Name</b>	<b>Date</b>	<b>M</b>	<b>Fault</b> <b>Mechanism</b>	<b>Epicentral</b> <b>Distance</b> <b>[km]</b>
600	286	ST223	Umbria Marche	26/09/1997	6	normal	22
6960	473	ST3266	Izmit (aft.)	13/09/1999	5.8	oblique	27
1726	561	ST549	Adana	27/06/1998	6.3	strike slip	30
335	158	ST121	Alkion	25/02/1981	6.3	normal	25
386	176	ST152	Lazio Abruzzo (aft.)	11/05/1984	5.5	normal	24
648	292	ST221	Umbria Marche (aft.)	14/10/1997	5.6	normal	13
6975	473	ST3272	Izmit (aft.)	13/09/1999	5.8	oblique	26

**Table 3.** Essential record returned by REXEL [53].

		Fib Bulletin n. 43	CNR 10025/84	Tassios, Vintzeleou		MODEL CODE 2010	Negro, Toniolo	Psycharis, Mouzakis		Soroushian
				<i>spalling</i>	<i>cyclic behaviour</i>		<i>spalling</i>	<i>small rotations</i>	<i>large rotations</i>	<i>spalling</i>
$T_R$ [years]	KL 1	5	2				5			
	KL 2									
	KL 3									
$I_R$	KL 1	0.155	0.11				0.155			
	KL 2									
	KL 3									

**Table 4.** Seismic risk index for linear dynamical analyses for *Model 3* (with dowel pins).

<i>Model 1 (cylindrical hinge)</i>					<i>Model 2 (spherical hinge)</i>				
Ductile mechanisms			Brittle mechanisms		Ductile mechanisms			Brittle mechanisms	
$T_R$ [years]	KL 1	40	>475		30			>475	
	KL 2								
	KL 3								
$I_R$	KL 1	0.363	>1.0		0.322			>1.0	
	KL 2								
	KL 3								

**Table 5.** Seismic risk index for linear dynamical analyses for *Models 1* and *2*.

		Fib Bulletin n. 43	CNR 10025/84	Tassios, Vintzeleou		MODEL CODE 2010	Negro, Toniolo	Psycharis, Mouzakis		Soroushian
				<i>spalling</i>	<i>cyclic behaviour</i>		<i>spalling</i>	<i>small rotations</i>	<i>large rotations</i>	<i>spalling</i>
$T_R$ [years]	KL 1	20	25	5	15	25	10	20	15	35
	KL 2									
	KL 3									
$I_R$	KL 1	0.273	0.299	0.155	0.243	0.299	0.205	0.273	0.243	0.343
	KL 2									
	KL 3									

**Table 6.** Seismic risk index for nonlinear static analyses for models with dowel pins (*Model 3*).

		<b>Model 1 (cylindrical hinge)</b>		<b>Model 2 (spherical hinge)</b>	
		Ductile mechanisms	Brittle mechanisms	Ductile mechanisms	Brittle mechanisms
<b>T<sub>R</sub></b> <b>[years]</b>	<b>KL 1</b>	35	>475	35	250 - global
	<b>KL 2</b>	55			
	<b>KL 3</b>	140			
<b>I<sub>R</sub></b>	<b>KL 1</b>	0.343	>1.0	0.343	0.8
	<b>KL 2</b>	0.413			
	<b>KL 3</b>	0.606			

**Table 7.** Seismic risk index for nonlinear static analyses for *Models 1* and *2*.